



1 **Seasonal study of stable carbon and nitrogen isotopic composition**
2 **in fine aerosols at a Central European rural background station**

3
4 Petr Vodička^{1,2}, Kimitaka Kawamura¹, Jaroslav Schwarz², Bhagawati Kunwar¹, Vladimír
5 Ždímal²

6
7 ¹ Chubu Institute for Advanced Studies, Chubu University, 1200 Matsumoto-cho, Kasugai 487–8501, Japan

8 ² Institute of Chemical Process Fundamentals of the Czech Academy of Science, Rozvojová 2/135, 165 02, Prague
9 6, Czech Republic

10 *Correspondence to:* vodicka@icpf.cas.cz (P. Vodička), kkawamura@isc.chubu.ac.jp (K. Kawamura)

11
12 **Abstract.** Determinations of stable carbon isotope ratios ($\delta^{13}\text{C}$) of total carbon (TC) and nitrogen
13 isotope ratios ($\delta^{15}\text{N}$) of total nitrogen (TN) were carried out for fine aerosol particles (PM₁) collected
14 on a daily basis at a rural background site in Košetice (Central Europe) between 27 September 2013
15 and 9 August 2014 (n=146). We found a seasonal pattern for both $\delta^{13}\text{C}$ and $\delta^{15}\text{N}$. The seasonal variation
16 in $\delta^{15}\text{N}$ was more pronounced, with ¹⁵N-depleted values (av. $13.1\pm 4.5\text{‰}$) in winter and ¹⁵N-enriched
17 values ($25.0\pm 1.6\text{‰}$) in summer. Autumn and spring are transition periods when the isotopic
18 composition gradually changed due to different sources and the ambient temperature. The seasonal
19 variation in $\delta^{13}\text{C}$ was less pronounced but more depleted in ¹³C in summer ($-27.8\pm 0.4\text{‰}$) compared to
20 winter ($-26.7\pm 0.5\text{‰}$).

21 Major controls of the seasonal dependencies were found based on a comparative analysis with water-
22 soluble ions, organic carbon, elemental carbon, trace gases and meteorological parameters (mainly
23 ambient temperature). A comparison of $\delta^{15}\text{N}$ with NO_3^- , NH_4^+ and organic nitrogen (OrgN) revealed
24 that although a higher content of NO_3^- was associated with a decrease in $\delta^{15}\text{N}$ values in TN, NH_4^+ and
25 OrgN had the opposite influences. The highest concentrations of nitrate, mainly represented by NH_4NO_3 ,
26 originated from the emissions from biomass burning, leading to lower $\delta^{15}\text{N}$ values of approximately
27 14‰ in winter. During spring, the percentage of NO_3^- in PM₁ decreased, and ¹⁵N enrichment was
28 probably driven by equilibrium exchange between the gas and aerosol phases ($\text{NH}_3(\text{g}) \leftrightarrow \text{NH}_4^+(\text{p})$) as
29 supported by the increased ambient temperature. This equilibrium was suppressed in early summer
30 when the $\text{NH}_4^+/\text{SO}_4^{2-}$ molar ratios reached 2, and nitrate partitioning in aerosol was negligible. During
31 summer, kinetic reactions probably were the primary processes as opposed to gas-aerosol equilibrium
32 on a nitrogen level. However, summertime $\delta^{15}\text{N}$ values were some of the highest observed, probably
33 suggesting the aging of ammonium sulfate and OrgN aerosols. Such aged aerosols can be coated by
34 organics in which ¹³C enrichment takes place by photooxidation process. This result was supported by
35 the positive correlation of $\delta^{13}\text{C}$ with temperature and ozone, as observed in the summer season.



36 During winter, we observed an event with the lowest $\delta^{15}\text{N}$ and highest $\delta^{13}\text{C}$ values. The winter *Event*
37 was connected with prevailing southeast winds. Although higher $\delta^{13}\text{C}$ values probably originated from
38 biomass burning particles, the lowest $\delta^{15}\text{N}$ values were associated with agriculture emissions of NH_3
39 under low temperature conditions that were below 0°C .

40

41 1. Introduction

42

43 Key processes in the atmosphere, which are involved with climate changes, air quality, rain events
44 (Fuzzi et al., 2015) or visibility (Hyslop, 2009), are strongly influenced by aerosols. Because these
45 processes are still insufficiently understood, they are studied intensively. One approach to explore
46 chemical processes taking place in atmospheric aerosols is the application of stable carbon ($\delta^{13}\text{C}$) and
47 nitrogen ($\delta^{15}\text{N}$) isotope ratios. These isotopes can provide unique information on source emissions
48 together with physical and chemical processes in the atmosphere (Gensch et al., 2014; Kawamura et al.,
49 2004), as well as atmospheric history (Dean et al., 2014). Isotopic composition is affected by both
50 primary emissions (e.g., Heaton, 1990; Widory, 2006) and secondary processes (e.g., Fisseha et al.,
51 2009b; Walters et al., 2015a). Both $\delta^{13}\text{C}$ and $\delta^{15}\text{N}$ values are influenced by kinetic and equilibrium
52 isotope fractionation that takes place in the atmosphere. In the case of nitrogen, ^{15}N is generally depleted
53 in gas phase precursors (ammonia, nitrogen oxides) but is more enriched in ions (NH_4^+ , NO_3^-) in rainfall
54 and most enriched in particulate matter and dry deposition (Heaton et al., 1997). In the case of carbon,
55 the major form is organic carbon (OC), which is composed of large numbers of organic compounds
56 where isotope fractionations via the kinetic isotope effect (KIE) usually dominating the partitioning
57 between gas and aerosol (liquid/solid) phases (Gensch et al., 2014).

58

59 Many studies have been conducted on $\delta^{13}\text{C}$ and $\delta^{15}\text{N}$ in particulate matter (PM) in Asia (e.g., Kundu et
60 al., 2010; Pavuluri et al., 2015b; Pavuluri and Kawamura, 2017) and America (e.g., Martinelli et al.,
61 2002; Savard et al., 2017). However, only few studies have been performed in Europe. European isotope
62 studies on aerosols mainly involve the analysis of $\delta^{15}\text{N}$ in NO_3^- and/or NH_4^+ . Widory (2007) published
63 a broad study on $\delta^{15}\text{N}$ in TN in PM10 samples from Paris, focusing on seasons (winter vs. summer)
64 with some specific sources. Freyer (1991) reported the seasonal variation in $\delta^{15}\text{N}$ of nitrate in aerosols
65 and rainwater as well as gaseous HNO_3 at a moderately polluted urban area in Jülich (Germany).
66 Yeatman et al. (2001a, 2001b) conducted analyses of $\delta^{15}\text{N}$ in NO_3^- and NH_4^+ at two coastal sites from
67 Weybourne, England, and Mace Head, Ireland, focusing on the effects of possible sources and aerosol
68 size segregation on their formation processes and isotopic enrichment. More recently, Ciężka et al.
69 (2016) reported one-year observations of $\delta^{15}\text{N}$ in NH_4^+ and ions in precipitation at an urban site in
70 Wrocław, Poland, whereas Beyn et al. (2015) reported seasonal changes in $\delta^{15}\text{N}$ in NO_3^- in wet and dry
71 deposition at a coastal and an urban site in Germany to evaluate nitrogen pollution levels.



72 Studies on $\delta^{13}\text{C}$ at European sites have been focused more on urban aerosols. Fisseha et al. (2009) used
73 stable carbon isotopes to determine the sources of urban carbonaceous aerosols in Zurich, Switzerland,
74 during winter and summer. Similarly, Widory et al. (2004) used $\delta^{13}\text{C}$ of TC, together with an analysis
75 of lead isotopes, to study the origin of aerosol particles in Paris (France). Górká et al. (2014) used $\delta^{13}\text{C}$
76 in TC together with PAH analyses for the determination of sources of PM10 organic matter in Wrocław,
77 Poland, during vegetative and heating seasons. Masalaite et al. (2015) used an analysis of $\delta^{13}\text{C}$ in TC
78 on size-segregated urban aerosols to elucidate carbonaceous PM sources in Vilnius, Lithuania. Fewer
79 studies have been conducted on $\delta^{13}\text{C}$ in aerosols in rural and remote areas of Europe. In the 1990s,
80 Pichlmayer et al. (1998) conducted an isotope analysis in snow and air samples for the characterization
81 of pollutants at high-alpine sites in Central Europe. Recently, Martinsson et al. (2017) published
82 seasonal observations of $\delta^{13}\text{C}$ in TC of PM10 at a rural background station in Vavíhill in southern
83 Sweden based on 25 weekly samples.

84

85 These $\delta^{13}\text{C}$ and $\delta^{15}\text{N}$ studies show the potential of these isotopes to characterize aerosol types and the
86 chemical processes that take place in them. To broaden this isotope approach over the European
87 continent, we present seasonal variations in $\delta^{13}\text{C}$ of total carbon (TC) and $\delta^{15}\text{N}$ of total nitrogen (TN)
88 in the PM1 fraction of atmospheric aerosols at a rural background site in Central Europe. To the best of
89 our knowledge, this is the first seasonal study of these isotopes in this location, and it is one of the most
90 comprehensive isotope studies of a fine fraction of aerosols.

91

92 **2. Materials and methods**

93 **2.1. Measurement site**

94

95 The Košetice observatory is the specialized workplace of the Czech Hydrometeorological Institute
96 (CHMI), which is focused on monitoring the quality of the environment (Váňa and Dvorská, 2014).
97 The site is located in the Czech Highlands (49°34'24.13" N, 15°4'49.67" E, 534 m ASL) and is
98 surrounded by an agricultural landscape and forests, out of range of major sources of pollution with a
99 very low frequency of traffic. The observatory is officially classified as a Central European rural
100 background site, which is part of the EMEP, ACTRIS, and GAW networks. A characterization of the
101 station in terms of the chemical composition of fine aerosols during different seasons and air masses is
102 presented by Schwarz et al. (2016) and longtime trends by Mbengue et al. (2018) and Pokorná et al.
103 (2018). As part of a monitoring network operated by the CHMI, the site is equipped with an automated
104 monitoring system that provides meteorological data (wind speed and direction, relative humidity,
105 temperature, pressure, and solar radiation) and the concentrations of gaseous pollutants (SO_2 , CO, NO,
106 NO_2 , NO_x and O_3).

107



108 2.2. Sampling and weighing

109

110 Aerosol samples ($n = 146$) were collected for 24 h every two days from September 27, 2013, to August
111 9, 2014, using a Leckel sequential sampler SEQ47/50 equipped with a PM1 sampling inlet. Some gaps
112 in sampling were caused by outages and maintenance to the sampler. The sampler was loaded with pre-
113 baked (3 h, 800°C) quartz fiber filters (Tissuequartz, Pall, 47 mm), and the flow rate of 2.3 m³/h was
114 used. In addition, field blanks ($n = 7$) were also taken for an analysis of the contribution of absorbable
115 organic vapors.

116

117 The mass of PM1 was measured by gravimetric analysis of each quartz filter before and after the
118 sampling with a microbalance that had ± 1 μg sensitivity (Sartorius M5P, Sartorius AG, Göttingen,
119 Germany). The weighing of samples was performed at 20 ± 1 °C and 50 ± 3 % relative humidity after
120 equilibration for 24 h.

121

122 2.3. Determination of TC, TN and their stable isotopes

123

124 For the TC and TN analyses, small filter discs (area 0.5 cm², 1.13 cm² or 2.01 cm²) were placed in a
125 pre-cleaned tin cup, shaped into a small marble using a pair of tweezers, and introduced into the
126 elemental analyzer (EA; Flash 2000, Thermo Fisher Scientific) using an autosampler. Inside the EA,
127 samples were first oxidized in a quartz column heated at 1000°C, in which tin marble burns (~1400°C)
128 and oxidizes all carbon and nitrogen species to CO₂ and nitrogen oxides, respectively. In the second
129 quartz column, heated to 750°C, nitrogen oxides were reduced to N₂. Evolved CO₂ and N₂ were
130 subsequently separated on a gas chromatographic column, which was installed in EA, and measured
131 with a thermal conductivity detector for TC and TN. Parts of CO₂ and N₂ were then transferred into an
132 isotope ratio mass spectrometer (IRMS; Delta V, Thermo Fisher Scientific) through a ConFlo IV
133 interface to monitor the ¹⁵N/¹⁴N and ¹³C/¹²C ratios.

134

135 An acetanilide external standard (from Thermo-electron-corp.) was used to determine the calibration
136 curves before every set of measurements for the calculation of the right values of TC, TN and their
137 isotopic ratios. The $\delta^{15}\text{N}$ and $\delta^{13}\text{C}$ values of the acetanilide standard were 11.89‰ (relative to the
138 atmospheric nitrogen) and -27.26‰ (relative to Vienna Pee Dee Belemnite standard), respectively.
139 Subsequently, the $\delta^{15}\text{N}$ of TN and $\delta^{13}\text{C}$ of TC were calculated using the following equations:

140

$$141 \quad \delta^{15}\text{N} (\text{‰}) = \left[\frac{(^{15}\text{N}/^{14}\text{N})_{\text{sample}}}{(^{15}\text{N}/^{14}\text{N})_{\text{standard}}} - 1 \right] * 1000$$

$$142 \quad \delta^{13}\text{C} (\text{‰}) = \left[\frac{(^{13}\text{C}/^{12}\text{C})_{\text{sample}}}{(^{13}\text{C}/^{12}\text{C})_{\text{standard}}} - 1 \right] * 1000$$

143



144 **2.4. Ion chromatography**

145

146 Quartz filters were further analyzed by using a Dionex ICS-5000 (Thermo Scientific, USA) ion
147 chromatograph (IC). The samples were extracted using ultrapure water with conductivity below 0.08
148 $\mu\text{S/m}$ (Ultrapur, Watrex Ltd., Czech Rep.) for 0.5 h using an ultrasonic bath and 1 h using a shaker. The
149 solution was filtered through a Millipore syringe filter with 0.22- μm porosity. The filtered extracts were
150 then analyzed for both anions (SO_4^{2-} , NO_3^- , Cl^- , NO_2^- and oxalate) and cations (Na^+ , NH_4^+ , K^+ , Ca^{2+} and
151 Mg^{2+}) in parallel. The anions were analyzed using an anion self-regenerating suppressor (ASRS 300)
152 and an IonPac AS11-HC (2 x 250 mm) analytical column and detected with a Dionex conductivity
153 detector. For cations, a cation self-regenerating suppressor (CSRS ULTRA II) and an IonPac CS18 (2
154 m x 250 mm) analytical column were used together with a Dionex conductivity detector. The separation
155 of anions was conducted using 25 mM KOH as an eluent at a flow rate of 0.38 ml/min, and the
156 separation of cations was conducted using 25 mM methanesulfonic acid at 0.25 ml/min.

157

158 The sum of nitrate and ammonium nitrogen was in good agreement with measured TN (Fig. S1 in
159 Supplementary Information (SI)), and based on the results of TN, NO_3^- and NH_4^+ , organic nitrogen
160 (OrgN) was also calculated using following equation (Wang et al., 2010): $\text{OrgN} = \text{TN} - 14 \cdot [\text{NO}_3^-/62 +$
161 $\text{NH}_4^+/18]$.

162

163 **2.5. EC/OC analysis**

164

165 Online measurements of organic and elemental carbon (OC and EC) in aerosols were provided in
166 parallel to the aerosol collection on quartz filters mentioned above by a field semionline OC/EC
167 analyzer (Sunset Laboratory Inc., USA) connected to a PM1 inlet. The instrument was equipped with a
168 carbon parallel-plate denuder (Sunset Lab.) to remove volatile organic compounds to avoid a positive
169 bias in the measured OC. Samples were taken at 4 h intervals, including the thermal-optical analysis,
170 which lasts approximately 15 min. The analysis was performed using the shortened EUSAAR2
171 protocol: step [gas] temperature [$^{\circ}\text{C}$]/duration [s]: He 200/90, He 300/90, He 450/90, He 650/135, He-
172 Ox. 500/60, He-Ox. 550/60, He-Ox. 700/60, He-Ox. 850/100 (Cavalli et al., 2010). Automatic optical
173 corrections for charring were made during each measurement, and a split point between EC and OC
174 was detected automatically (software: RTCalc526, Sunset Lab.). Instrument blanks were measured once
175 per day at midnight, and they represent only a background instrument signal without any reflection on
176 concentrations. Control calibrations using a sucrose solution were made before each change of the filter
177 (ca. every 2nd week) to check the stability of instruments. The 24 h averages with identical measuring
178 times, such as on quartz filters, were calculated from acquired 4 h data. The sum of EC and OC provided
179 the TC concentrations, which were consistent with TC values measured by EA (see Fig. S2 in SI).



180

181 **2.6. Spearman correlation calculations**

182

183 Spearman correlation coefficients (r) were calculated using R statistical software (ver. 3.3.1).
184 Correlations were calculated for the annual dataset (139 samples), separately for each season (autumn
185 - 25, winter - 38, spring - 43, and summer - 33 samples), and the winter *Event* (7 samples). Data from
186 the winter *Event* were excluded from the annual and winter datasets for the correlation analysis.
187 Correlations with p -values over 0.05 were taken as statistically insignificant.

188

189 **3. Results and discussion**

190

191 The time series of TN, TC and their isotope ratios ($\delta^{15}\text{N}$ and $\delta^{13}\text{C}$) for the whole measurement campaign
192 are depicted in Fig. 1. Sampling gaps in autumn and at the end of spring are caused by servicing or
193 outages of the sampler; however, 146 of the samples between September 27, 2013, and August 9, 2014,
194 are enough for a seasonal study. In Fig. 1, the winter *Event* is highlighted, which has divergent values,
195 especially for $\delta^{15}\text{N}$, and is discussed in detail in section 3.4.

196

197 Table 1 summarizes the results for the four seasons: autumn (Sep–Nov), winter (Dec–Feb), spring
198 (Mar–May) and summer (Jun–Aug). The higher TN concentrations were observed in spring (max. 7.59
199 $\mu\text{gN m}^{-3}$), while the higher TC concentrations were obtained during the winter *Event* (max. 13.6 μgC
200 m^{-3}). Conversely, the lowest TN and TC concentrations were observed in summer (Fig. 1).

201

202 Figure 2 shows relationships between TC and TN and their stable isotopes for one year. The correlation
203 between TC and TN is significant ($r=0.70$), but during higher concentration events, this dependence
204 can be split due to the different origins of these components. The highest correlations between TC and
205 TN were obtained during transition periods in autumn (0.85) and spring (0.80). Correlations between
206 TC and TN in winter (0.43) and in summer (0.37) were weaker but still statistically significant ($p<0.05$).
207 As seen in the TC/TN ratios (Table 1), seasonal TC/TN averages fluctuate, but their medians have
208 similar values for autumn, winter and spring, while the summer value is higher (3.45) and roughly
209 points to different aerosol composition in comparison with other seasons. However, seasonal
210 differences between TC/TN ratios are not as large as those in other works (e.g., Agnihotri et al., 2011),
211 and thus, this ratio itself does not provide much information about aerosol sources.

212

213 The correlation between $\delta^{13}\text{C}$ and $\delta^{15}\text{N}$ (Fig. 2, right) is also significant but negative (-0.71). However,
214 there is a statistically significant correlation for spring only (-0.54), while in other seasons, correlations



215 are statistically insignificant (autumn: -0.29, winter: -0.11 and summer: 0.07). This result shows that
216 significant and related changes in the isotopic composition of nitrogen together with carbon occur
217 especially in spring, while there are stable sources of particles during winter and summer. The winter
218 *Event* measurements show the highest $\delta^{13}\text{C}$ values and the lowest $\delta^{15}\text{N}$ values, but they are still in line
219 with the linear fitting of all annual data (Fig. 2, right).

220

221 3.1. Total nitrogen and its $\delta^{15}\text{N}$

222

223 The $\delta^{15}\text{N}$ values are stable in winter at approximately 15‰, with the exception of the winter *Event*,
224 which deviated by an average of 13‰. In summer, the $\delta^{15}\text{N}$ shows strong enrichment of ^{15}N in
225 comparison with winter, resulting in an average value of 25‰. During the spring period, we observe a
226 slow increase in $\delta^{15}\text{N}$ from April to June (Fig. 1), indicating a gradual change in nitrogen chemistry in
227 the atmosphere. During autumn, a gradual change is not obvious because of a lack of data in a
228 continuous time series. Year round, $\delta^{15}\text{N}$ ranged from 0.6‰ to 28.2‰. Such a large range may originate
229 from the limited number of main compounds containing nitrogen in aerosols, which is specifically
230 present in the form of NO_3^- , NH_4^+ and/or organic nitrogen (OrgN), and thus, the final $\delta^{15}\text{N}$ value in TN
231 can be formulated by the following equation:

$$232 \delta^{15}\text{N}_{\text{TN}} = \delta^{15}\text{N}_{\text{NO}_3^-} * f_{\text{NO}_3^-} + \delta^{15}\text{N}_{\text{NH}_4^+} * f_{\text{NH}_4^+} + \delta^{15}\text{N}_{\text{OrgN}} * f_{\text{OrgN}}$$

233 where $f_{\text{NO}_3^-} + f_{\text{NH}_4^+} + f_{\text{OrgN}} = 1$ and f represents the fractions of nitrogen from NO_3^- , NH_4^+ and OrgN in
234 TN, respectively. The highest portion of nitrogen is contained in NH_4^+ (54 % of TN year-round),
235 followed by OrgN (27 %) and NO_3^- (19 %). While the NH_4^+ content in TN is seasonally stable (51-
236 58 %, Table 1), the NO_3^- content is seasonally dependent – higher in winter, similarly balanced in spring
237 and autumn, and very low in summer, when the dissociation of NH_4NO_3 plays an important role, and
238 its nitrogen is partitioned from the aerosol phase to the gas phase (Stelson et al., 1979).

239

240 The seasonal trend of $\delta^{15}\text{N}$ in TN, with the lowest values in winter and highest in summer, has been
241 observed in other studies from urban Paris (Widory, 2007), rural Brazil (Martinelli et al., 2002), East
242 Asian Jeju Island (Kundu et al., 2010) and rural Baengnyeong Island (Park et al., 2018) sites in Korea.
243 However, different seasonal trends of $\delta^{15}\text{N}$ in TN in Seoul (Park et al., 2018) show that such seasonal
244 variation does not always occur.

245

246 Figure 3 shows changes in $\delta^{15}\text{N}$ values as a function of the main nitrogen components in TN, with
247 different colors for different days. There are two visible trends for a type of nitrogen. Although ^{15}N is
248 more depleted with increasing contents of NO_3^- in TN, the opposite is true for NH_4^+ and OrgN. The
249 strongest dependence of most of the bulk data is expressed by a strong negative correlation between
250 $\delta^{15}\text{N}$ and the share of NO_3^- in TN (Fig. 3). In all cases, the dependence during the winter *Event* is



251 completely opposite to the rest of the bulk data (Fig. 3) showing different processes on $\delta^{15}\text{N}$ formation,
252 which is highlighted by a very strong positive correlation between $\delta^{15}\text{N}$ and NO_3^- -N/TN (0.98). This
253 point will be discussed in section 3.4.

254

255 Considering the individual nitrogen components, several studies (Freyer, 1991; Kundu et al., 2010;
256 Yeatman et al., 2001b) show seasonal trends of $\delta^{15}\text{N}$ of NO_3^- , with the lowest $\delta^{15}\text{N}$ in summer and the
257 highest in winter. Savard et al. (2017 and references therein) summarized four possible reasons for this
258 seasonality of $\delta^{15}\text{N}$ in NO_3^- , that is, (i) changes in emissions strength, (ii) influence of wind directions
259 in the relative contributions from sources with different isotopic composition, (iii) the effect of
260 temperature on isotopic fractionation and (iv) chemical transformations of nitrogen oxides over time
261 with a lower intensity of sunlight, which can lead to higher $\delta^{15}\text{N}$ values of atmospheric nitrate during
262 winter months, as shown by Walters et al. (2015a). In the case of our data, mixing of all of these factors
263 probably had an influence on the nitrate isotopic composition during different parts of the year.

264

265 Conversely, Kundu et al. (2010) reported higher $\delta^{15}\text{N}$ values of NH_4^+ in summer than in winter and
266 generally reported higher $\delta^{15}\text{N}$ values in NH_4^+ than in NO_3^- except for winter. In sum, the contribution
267 of NH_4^+ to $\delta^{15}\text{N}$ overwhelms the contribution of NO_3^- to $\delta^{15}\text{N}$. Additionally, TN is composed of NH_4^+ ,
268 NO_3^- and OrgN. In Fig. 3, we can observe the enrichment of ^{15}N in TN in summer when the lowest
269 NO_3^- contribution occurs. Thus, higher values of $\delta^{15}\text{N}$ in TN in summer are mainly caused by NH_4^+
270 originating from $(\text{NH}_4)_2\text{SO}_4$, OrgN and ammonium salts of organic acids.

271

272 Furthermore, in summer, we observed one of the largest enrichments of ^{15}N in TN aerosols in
273 comparison with other studies (Kundu et al., 2010 and references therein), which may be due to several
274 reasons. First, the works mentioned above mainly studied total suspended particles (TSP) aerosols;
275 however, we focus on the fine PM1 fraction, which should be more reactive than the coarse fraction
276 and consequently result in a higher abundance of ^{15}N during the gas/particle partitioning of NH_3 and
277 NH_4^+ . Second, the fine aerosol fraction of the Aitken mode persists for a longer period of time in the
278 atmosphere than the coarse fraction, which is also a factor leading to higher ^{15}N enrichment. Indeed,
279 Mkoma et al. (2014) reported average higher $\delta^{15}\text{N}$ in TN in fine aerosols (17.4‰, PM2.5) in comparison
280 with coarse aerosols (12.1‰, PM10), and Freyer (1991) also reported higher $\delta^{15}\text{N}$ in NO_3^- (4.2‰ to
281 8‰) in fine aerosols ($< 3.5 \mu\text{m}$) in comparison with the coarse mode (-1.4‰ to 5.5‰). Third, a shorter
282 sampling time in this work (24 h) leads to the collection of samples with episodic values (see the winter
283 *Event*) that would be averaged (overlapped) over a longer time resolution (e.g., weekly samples).

284

285 Similarly, as in this study, the highest $\delta^{15}\text{N}$ values in TN were observed in a few studies from the Indian
286 region (Aggarwal et al., 2013; Bikkina et al., 2016; Pavuluri et al., 2010) where biomass burning is



287 common, and ambient temperatures are high. Therefore, in addition to the above reasons, temperature
288 also plays a significant role in ^{15}N enrichment. This point will be discussed in more detail in section 3.3.
289

290 Figure 4 shows the $\delta^{15}\text{N}$ in TN as a function of NO_3^- . The $\delta^{15}\text{N}$ shows a peak at approximately $14\pm 1\%$
291 with increasing nitrate concentrations. Assuming that NO_3^- in the fine aerosol fraction consists
292 predominantly of NH_4NO_3 (Harrison and Pio, 1983), it can be stated that nitrate at the Košetice site is
293 a source of nitrogen, with $\delta^{15}\text{N}$ values at approximately 14% , which is similar to the winter values of
294 $\delta^{15}\text{N}$ in NO_3^- in other studies. Specifically, Kundu et al. (2010) reported a winter average value of $\delta^{15}\text{N}$
295 in NO_3^- at $+15.9\%$ from a Pacific marine site at Gosan Island, South Korea, whereas Freyer (1991)
296 reported $+9.2\%$ in a moderately polluted site from Jülich, Germany. Yeatman et al. (2001) reported
297 approximately $+9\%$ from a Weybourne coastal site, UK. Park et al. (2018) reported 11.9% in Seoul
298 and 11.7% from a rural site in Baengnyeong Island, Korea.

299

300 Considering the $\delta^{15}\text{N}$ of nitrogen oxides, which are common precursors of particulate nitrate, we can
301 see that the $\delta^{15}\text{N}$ of nitrogen oxides generated by coal combustion (Felix et al., 2012; $+6$ to $+13\%$,
302 Heaton, 1990) or biomass burning ($+14\%$, Felix et al., 2012) are in a same range with our $\delta^{15}\text{N}$ during
303 the period of enhanced concentrations of NO_3^- . These $\delta^{15}\text{N}$ values of nitrogen oxides are also
304 significantly higher than those from vehicular exhaust (-13 to -2% Heaton, 1990; -19 to $+9\%$ Walters
305 et al., 2015b) or biogenic soil (-48 to -19% , Li and Wang, 2008). Thus, $\delta^{15}\text{N}$ values of approximately
306 14% (Fig. 4) are probably characteristic of fresh emissions from heating (both coal and biomass
307 burning) because these values are obtained during the domestic heating season.

308

309 The exponential curves in Fig. 4 represent a boundary in which the $\delta^{15}\text{N}$ values are migrating as a result
310 of enrichment or depletion of ^{15}N , which is associated with removal or loading of NO_3^- in aerosols.
311 These curves represent two opposite chemical processes, with a match at approximately 14% , which
312 showed a strong logarithmic correlation ($r=0.96$ during winter *Event*, green line, and -0.81 for the rest
313 of points, black line, Fig. S3). These results indicate a significant and different mechanism by which
314 nitrogen isotopic fractionation occurs in aerosols. In both cases, the decrease in nitrate leads to
315 exponential changes in the enrichment or depletion of ^{15}N from a value of approximately 14% . In the
316 case of enrichment, in addition to a higher proportion of NH_4^+ than NO_3^- , the dissociation process of
317 NH_4NO_3 can cause an increase in ^{15}N in TN during a period of higher ambient temperatures, as
318 hypothesized by Pavuluri et al. (2010).

319

320 OrgN has not been widely studied compared to particulate NO_3^- and NH_4^+ , although it represents a
321 significant fraction of TN (e.g., Jickells et al., 2013; Neff et al., 2002; Pavuluri et al., 2015). Figure 5
322 shows the relationship between $\delta^{15}\text{N}$ in TN and OrgN. Organic nitrogen consists organic compounds
323 containing nitrogen in water soluble and insoluble fractions. The majority of samples have a



324 concentration range of 0.1-0.5 $\mu\text{g m}^{-3}$ (gray highlight in Fig. 5), which can be considered as background
325 OrgN at the Košetice site. During the domestic heating season with the highest concentrations of NO_3^-
326 and NH_4^+ , we can observe a significant increase in OrgN with $\delta^{15}\text{N}$ again at approximately 14%, which
327 implies that the isotopic composition of OrgN is determined by the same process during maximal NO_3^-
328 concentrations, that is, emissions from domestic heating. In the case of emissions from combustion,
329 OrgN originates mainly from biomass burning (Jickells et al., 2013 and references therein), and thus,
330 elevated concentrations of OrgN (together with high NO_3^- and NH_4^+ conc.) may refer to this source. On
331 the other hand, looking at the trend of OrgN/TN in dependence on $\delta^{15}\text{N}$ (Fig. 3), it is more similar to
332 the trend of NH_4^+ -N/TN than NO_3^- -N/TN. Thus, it can be assumed that changes in the $\delta^{15}\text{N}$ in OrgN in
333 samples highlighted as a gray area in Fig. 5 are probably driven more by the same changes in NH_4^+
334 particles, and especially in summer with elevated OrgN in TN (Table 1).

335

336 3.2. Total carbon and its $\delta^{13}\text{C}$

337

338 The $\delta^{13}\text{C}$ of TC ranged between -25.4‰ and -28.9‰ (Fig. 6), which is similar but broader than the
339 range reported at a rural background site in Vavihill (southern Sweden, range -26.7 to -25.6‰,
340 Martinsson et al. (2017)), urban Wroclaw (Poland, range -27.6 to -25.3‰, Górká et al. (2014)), and
341 different sites (urban, coastal, forest) in Lithuania (East Europe, Masalaite et al., 2015, 2017) but similar
342 to those published by Fisseha et al. (2009) in Zurich. However, our $\delta^{13}\text{C}$ values are smaller than those
343 reported for coastal TSP aerosols from Okinawa (East Asia, range -24.2 to -19.5‰, Kunwar et al.
344 (2016)) or rural Tanzania (Central-East Africa, range -26.1 to -20.6‰ in $\text{PM}_{2.5}$, Mkoma et al. (2014)).
345 In fact, similar or different $\delta^{13}\text{C}$ values are widely reported in the northern and southern hemispheres
346 (Cachier, 1989), which can be explained by different distributions of C3 and C4 plants (Martinelli et
347 al., 2002), the influence of marine aerosols (Ceburnis et al., 2016), as well as different anthropogenic
348 sources (e.g., Widory et al., 2004). The $\delta^{13}\text{C}$ values at the Košetice site fall within the range common
349 to other European sites. The $\delta^{13}\text{C}$ values are significantly smaller than those of $\delta^{15}\text{N}$ due to a higher
350 number of carbonaceous compounds in the aerosol mixture whose isotope ratio overlaps each other.
351 However, it is possible to distinguish lower $\delta^{13}\text{C}$ values in summer (Table 1), which may indicate a
352 contribution from higher terrestrial plant emissions. Similarly, Martinsson et al. (2017) reported lower
353 $\delta^{13}\text{C}$ values in summer in comparison with other seasons, which they explain by high biogenic aerosol
354 contributions from C3 plants.

355

356 A comparison of $\delta^{13}\text{C}$ with TC in Fig. 6 shows an enhanced enrichment of ^{13}C at higher TC
357 concentrations. The lowest $\delta^{13}\text{C}$ values were observed in field blank samples (mean -29.2‰, n=7),
358 indicating that the lowest summer values in particulate matter were close to gas phase values. A similar
359 dependence of $\delta^{13}\text{C}$ on the TC concentration was observed by Fisseha et al. (2009), whereby winter ^{13}C



360 enrichment was associated with WSOC (water soluble organic carbon) that originated mainly from
361 wood combustion. Similarly, at the Košetice station, different carbonaceous aerosols were observed
362 during the heating season (Oct.–Apr.) than in summer (Mbengue et al., 2018; Vodička et al., 2015),
363 whereby winter aerosols were probably affected by not only biomass combustion but also burning of
364 coal (Schwarz et al., 2016), which can result in higher carbon contents and more ^{13}C enriched particles
365 (Widory, 2006). However, relatively low $\delta^{13}\text{C}$ values in our range (up to -28.9%) are caused by not
366 only sources of TC but also a the fact that fine particles are more ^{13}C depleted in comparison with coarse
367 particles (e.g., Masalaite et al., 2015; Skipitytė et al., 2016). Furthermore, based on the number of size
368 distribution measurements at the Košetice site, larger particles were observed in winter in comparison
369 with summer, even in the fine particle fraction (Zíková and Ždímal, 2013), which can also have an
370 effect on lower $\delta^{13}\text{C}$ values in summer.

371

372 3.3. Temperature dependence and correlations of $\delta^{15}\text{N}$ and $\delta^{13}\text{C}$ with other variables

373

374 Tables 2 and 3 show Spearman's correlation coefficients (r) of $\delta^{15}\text{N}$ and $\delta^{13}\text{C}$ with different variables
375 that may reflect some effects on these isotopes. In addition to year-round correlations, correlations for
376 each season, as well as for the *Event*, are presented separately.

377

378 Correlations of $\delta^{15}\text{N}$ in winter and summer are often opposite (see e.g., for TN -0.40 in winter vs. 0.36
379 in summer, for NH_4^+ -0.42 in winter vs. 0.40 in summer), indicating that changes in aerosol chemistry
380 at the nitrogen level are different in these seasons. Similarly, the contradictory dependence between
381 $\delta^{15}\text{N}$ and TN in summer and winter was observed by Widory (2007) on PM₁₀ samples from Paris and
382 was connected with secondary processes affecting the nitrogen chemistry that follows two distinct
383 pathways between ^{15}N enrichment (summer) and depletion (winter).

384

385 From a meteorological point of view, a significant correlation of $\delta^{15}\text{N}$ with temperature has been
386 obtained, indicating the influence of temperature on the nitrogen isotopic composition. Dependence of
387 $\delta^{15}\text{N}$ in TN on temperature (Fig. 7) is opposite to that observed by Freyer (1991) for $\delta^{15}\text{N}$ in NO_3^- ;
388 however, it is same to that observed by Ciężka et al. (2016) for $\delta^{15}\text{N}$ in NH_4^+ from precipitation. These
389 authors concluded that the isotope equilibrium exchange between nitrogen oxides and particulate
390 nitrates is temperature dependent and could lead to more ^{15}N enriched NO_3^- during the cold season
391 (Freyer et al., 1993; Savard et al., 2017). Although Savard et al. (2017) reported a similar negative $\delta^{15}\text{N}$
392 in NH_4^+ dependence at temperatures in Alberta (Canada), such as for NO_3^- , most studies (e.g.,
393 Kawashima and Kurahashi, 2011; Kundu et al., 2010) reported the opposite temperature dependence
394 for $\delta^{15}\text{N}$ in NH_4^+ because the NH_3 gas concentrations are more abundant during warm weather



395 conditions, and thus, isotopic equilibrium exchange $\text{NH}_3(\text{g}) \leftrightarrow \text{NH}_4^+(\text{p})$ leading to ^{15}N enrichment in
396 particles is more intensive.

397 All the considerations mentioned above indicate that a final relationship between $\delta^{15}\text{N}$ in TN and
398 temperature is driven by the prevailing nitrogen species, which is NH_4^+ in our case. A similar
399 dependence was reported by Pavuluri et al. (2010) between temperature and $\delta^{15}\text{N}$ in TN in Chennai
400 (India), where NH_4^+ strongly prevailed. They found the best correlation between $\delta^{15}\text{N}$ and temperature
401 during the colder period (range 18.4-24.5°C, avg. 21.2°C); however, during warmer periods, this
402 dependence was weakened. In our study, we observed the highest correlation of $\delta^{15}\text{N}$ with temperature
403 in autumn ($r=0.58$, temp. range -1.9 to 13.9°C, avg. 6.6°C), followed by spring ($r=0.52$, temp. range
404 1.5-18.7°C, avg. 9.3°C), but there was even a negative but insignificant correlation in summer ($r=-0.21$,
405 temp. range: 11.8-25.5°C, avg. 17.7°C). This result indicates that temperature plays an important role
406 in the enrichment/depletion of ^{15}N ; however, it is not determined by a specific temperature range but
407 rather the conditions for repeating the process of "evaporation/condensation", as shown by the
408 comparison with the work of Pavuluri et al. (2010). It is likely that isotopic fractionation caused by the
409 equilibrium reaction of $\text{NH}_3(\text{g}) \leftrightarrow \text{NH}_4^+(\text{p})$ reaches a certain level of enrichment under higher
410 temperature conditions in summer.

411

412 In summer, $\delta^{15}\text{N}$ correlates positively with NH_4^+ ($r=0.40$) and SO_4^{2-} (0.51), indicating a link with
413 $(\text{NH}_4)_2\text{SO}_4$ that is enriched by ^{15}N due to aging. Figure 8 shows a decreasing molar ratio of $\text{NH}_4^+/\text{SO}_4^{2-}$
414 with increasing ^{15}N enrichment, especially during spring, indicating a gradual uptake of ammonia in the
415 gas phase to aerosol phase. With a decreasing $\text{NH}_4^+/\text{SO}_4^{2-}$ molar ratio, there is also a visible decrease in
416 the nitrate content in aerosols (Fig. 8). However, when the $\text{NH}_4^+/\text{SO}_4^{2-}$ ratio approaches a value below
417 2, there is not enough available ammonia in the gas phase, leading to the exclusion of nitrate from the
418 aerosol phase, as well as to the disruption of the thermodynamic equilibrium between $\text{NH}_3(\text{g}) \leftrightarrow$
419 $\text{NH}_4^+(\text{p})$, which previously led to ^{15}N enrichment in the particles. In this context, we note that 25 out of
420 33 summer samples have molar $\text{NH}_4^+/\text{SO}_4^{2-}$ ratios below 2, and the remaining samples are
421 approximately 2, although the average relative abundance of NO_3^- in PM1 in those samples is very low
422 (ca. 1.7 %).

423

424 Recently, Silvern et al. (2017) reported that organic aerosols can play a role in modifying or retarding
425 the achievement of $\text{H}_2\text{SO}_4\text{-NH}_3$ thermodynamic equilibrium at $\text{NH}_4^+/\text{SO}_4^{2-}$ ratios of less than 2, even
426 when sufficient amounts of ammonia are present in the gas phase. Thus, an interaction between sulfates
427 and ammonia may be hindered such that organics coated with aged aerosols preferentially react (Liggio
428 et al., 2011). Indeed, we observed a positive (and significant) correlation between temperature and $\delta^{13}\text{C}$
429 ($r=0.39$) only in summer, whereas $\delta^{15}\text{N}$ vs. temperature is negative (-0.21), suggesting that the
430 thermodynamic equilibrium between $\text{NH}_3(\text{g})$ and nitrogen in particles was minimal or replaced by the
431 influence of organics in this season. Ammonia measurements directly at the Košetice site were carried



432 out until 2001, and they showed that the NH_3 concentrations in summer and winter were comparable
433 (http://portal.chmi.cz/files/portal/docs/uoco/isko/tab_roc/2000_enh/CZE/kap_18/kap_18_026.html),
434 which indirectly support the above hypothesis.

435

436 The summer positive correlations of $\delta^{13}\text{C}$ with ozone ($r=0.66$) and temperature (0.39) indicate oxidation
437 processes that can indirectly lead to carbon isotope enrichment. This result is also supported by the fact
438 that the content of oxalate in PM_{10} , measured by IC, was twice as high in spring and summer than in
439 winter and autumn. The influence of temperature on $\delta^{13}\text{C}$ in winter is opposite to that in the summer.
440 The winter negative correlation (-0.35) probably points to the evolution of more fresh emissions from
441 domestic heating with higher contents of ^{13}C during lower temperatures.

442

443 The whole year temperature dependence on $\delta^{13}\text{C}$ is the opposite of that observed for $\delta^{15}\text{N}$ (Fig. 7, left),
444 suggesting more ^{13}C -depleted products in summer. This result is probably connected with different
445 carbonaceous aerosols during winter (anthropogenic emissions from coal, wood and biomass burning
446 with the enrichment of ^{13}C) in comparison with the summer season (primary biogenic and secondary
447 organic aerosols with lower $\delta^{13}\text{C}$). The data of $\delta^{13}\text{C}$ in Fig. 7 are also more scattered, which indicates
448 that in the case of carbon, the isotopic composition depends more on sources than on temperature.

449

450 Correlations of $\delta^{13}\text{C}$ with OC are significant in all seasons; they are strongest in spring and weakest in
451 summer (Table 3). Correlations of $\delta^{13}\text{C}$ with EC, whose main source is combustion processes from
452 domestic heating and transportation, are significant ($r=0.61-0.88$) only during the heating season
453 (autumn–spring, see Table 3), while in summer, the correlation is statistically insignificant (0.28). Thus,
454 the isotopic composition of aerosol carbon at the Košetice station is not significantly influenced by EC
455 emitted from transportation, otherwise the year-round correlation between $\delta^{13}\text{C}$ and EC would also be
456 significant in summer. This result is consistent with positive correlations between $\delta^{13}\text{C}$ and gaseous
457 NO_2 , as well as particulate nitrate, which is also significant from autumn to spring, and this result is
458 also supported by the negative correlation of $\delta^{13}\text{C}$ with the EC/TC ratio ($r=-0.51$), which is significant
459 only in summer.

460

461 It should be mentioned that the wind directions during the campaign were similar, with the exception
462 of the winter season, when southeast (SE) winds prevailed (see Fig. S4 in SI). We did not observe any
463 specific dependence of isotopic values on wind directions, except for the *Event*.

464

465

466

467 **3.4. Winter Event**

468

469 The winter *Event* represents a period between January 23 and February 5, 2014, when enrichment of
470 ^{13}C and substantial depletion of ^{15}N occurred in PM1 (see Figs. 1 and 9 for details). We do not observe
471 any trends of the isotopic compositions of $\delta^{15}\text{N}$ and $\delta^{13}\text{C}$ with wind directions, except for the period of
472 the *Event* and one single measurement on 18th December 2013. Both the *Event* and the single
473 measurement are connected to SE winds through Vienna and the Balkan Peninsula (Fig. 10). More
474 elevated wind speeds with very stable SE winds are observed on the site with samples showing the most
475 ^{15}N depleted values at the end of the *Event* (Fig. 9). Stable weather conditions and the homogeneity of
476 the results indicate a local or regional source, which is probably associated with emissions of sulfates
477 (Fig. S5), which are not sufficiently mixed at this time.

478

479 Although the *Event* contains only 7 samples, high correlations are obtained for $\delta^{15}\text{N}$ and $\delta^{13}\text{C}$ (Tables 2
480 and 3). Generally, correlations of $\delta^{15}\text{N}$ with several parameters during the *Event* are opposite to those
481 of the four seasons, indicating the exceptional nature of these aerosols from a chemical point of view.
482 During the *Event*, $\delta^{15}\text{N}$ correlates positively with NO_3^- ($r=0.96$) and $\text{NO}_3^-/\text{N}/\text{TN}$ (0.98), with large
483 values of $\delta^{15}\text{N}$ at approximately 14‰, which we previously interpreted as the emissions from domestic
484 heating by coal and/or biomass burning. Positive correlations of $\delta^{13}\text{C}$ with oxalate and potassium (both
485 0.93) and the negative correlation with temperature (-0.79) also show that the *Event* is associated with
486 emissions from combustion.

487

488 In contrast, we find that most $\delta^{15}\text{N}$ values with a depletion of ^{15}N are associated with enhanced NH_4^+
489 contents (70-80 %) and the almost total absence of NO_3^- nitrogen (see Figs. 3 and 4). Although some
490 content of OrgN is detected during the *Event* (Fig. 3), the correlation between $\delta^{15}\text{N}$ and OrgN/TN is not
491 significant (Table 2). This result shows that nitrogen with the lowest $\delta^{15}\text{N}$ values is mainly connected
492 with NH_4^+ , which is supported by a strong negative correlation between $\delta^{15}\text{N}$ and NH_4^+/TN (-0.86).
493 Assuming that nitrogen in particles mainly originates from gaseous nitrogen precursors via gas-to-
494 particle conversion (e.g., Wang et al., 2017) during the *Event*, we should expect the nitrogen to originate
495 mainly from NH_3 with depleted ^{15}N but not nitrogen oxides. Agricultural emissions from both fertilizer
496 application and animal waste are such sources of NH_3 emissions (Felix et al., 2013). Considering
497 possible agriculture emission sources, there exist several collective farms, with both livestock (mainly
498 cows, Holsteins cattle) and crop production in the SE direction from the Košetice observatory – namely,
499 Agropodnik Košetice (in 3.4 km distance), Agrodam Hořepník (6.8 km) and Agrorev Červená Řečice
500 (9.5 km). Skipitytė et al. (2016) reported lower $\delta^{15}\text{N}$ values of TN (+1 to +6‰) for agriculture-derived
501 particulate matter of poultry farms, which are close to our values obtained during the *Event*.

502



503 The $\delta^{15}\text{N}$ values from the *Event* are associated with an average temperature of below 0°C (Figs. 7 and
504 9). Savard et al. (2017) observed the lowest values of $\delta^{15}\text{N}$ in NH_3 with temperatures below -5°C , and
505 the NH_4^+ particles that were simultaneously sampled were also isotopically lighter compared to the
506 samples collected under higher temperature conditions. They interpreted this result as the preferential
507 dry deposition of heavier isotopic $^{15}\text{NH}_3$ species during the cold period, whereas the remaining lighter
508 $^{14}\text{NH}_3$ species in the atmosphere, lead to lighter NH_4^+ in particles. Moreover, the removal of NH_3 by
509 dry deposition also leads to a non-equilibrium state between the gas and aerosol phases. Such an absence
510 of equilibrium exchange of NH_3 between the gas and liquid/solid phases is supported by a $\text{NH}_4^+/\text{SO}_4^{2-}$
511 molar ratio below 2 for the three most ^{15}N depleted samples (Fig. 8). In such conditions, nitrate
512 partitioning in PM is negligible, and unidirectional reactions of lighter NH_3 isotope with H_2SO_4 in the
513 atmosphere are strongly preferred due to the kinetic isotope effect, which is (after several minutes)
514 followed by enrichment of the nitrogen due to the newly established equilibrium (Heaton et al., 1997).
515 Based on laboratory experiments, Heaton et al. (1997) estimated the isotopic enrichment factor between
516 gas NH_3 and particle NH_4^+ , $\epsilon_{\text{NH}_4-\text{NH}_3}$, to be +33‰. Savard et al. (2017) reported an isotopic difference
517 ($\Delta\delta^{15}\text{N}$) between NH_3 (g) and particulate NH_4^+ as a function of temperature, whereas $\Delta\delta^{15}\text{N}$ for a
518 temperature of approximately 0°C was approximately 40‰. In both cases, after subtraction of these
519 values (33 or 40‰) from the $\delta^{15}\text{N}$ values of the measured *Event*, we obtain values between
520 approximately -28 to -40‰, which are in a range of $\delta^{15}\text{N}$ - NH_3 (g) measured for agricultural emissions.
521 These values are especially in good agreement with $\delta^{15}\text{N}$ of NH_3 derived from cow waste (ca. -22 to -
522 38‰, Felix et al., 2013).

523

524 Thus, in case of the *Event*, we probably observe PM representing a mixture of aerosols from household
525 heating characterized by higher amounts of NO_3^- and $\delta^{15}\text{N}$ in TN (ca. 14‰), which are gradually
526 replaced by ^{15}N -depleted agricultural aerosols. Results of the whole process from low temperatures that
527 first support dry deposition of NH_3 followed by unidirectional (kinetic) reaction of lighter isotope
528 $\text{NH}_3(\text{g}) \rightarrow \text{NH}_4^+(\text{p})$ originate mainly from agricultural sources in the SE direction from the Košetice
529 station.

530

531 If the four lowest values of $\delta^{15}\text{N}$ mainly represent agricultural aerosols, then the $\delta^{13}\text{C}$ values from the
532 same samples should also be characteristic of agricultural sources. In this case, the $\delta^{13}\text{C}$ values ranging
533 from -25.4 to -26.2‰ belong to the most ^{13}C enriched fine aerosols at the Košetice site. However,
534 similar $\delta^{13}\text{C}$ values were reported by Widory (2006) for particles from coal combustion. Skipitytė et al.
535 (2016) reported a mean value of $\delta^{13}\text{C}$ in TC ($-23.7 \pm 1.3\%$) for PM1 particles collected on a poultry farm,
536 and they suggested the litter as a possible source for the particles. Thus, in the case of $\delta^{13}\text{C}$ during the
537 *Event* we observed, emissions either from domestic heating and/or agricultural sources are responsible
538 for the ^{13}C values.

539



540 4. Summary and Conclusions

541

542 Based on the analysis of year-round data of stable carbon and nitrogen isotopes, we extracted some
543 important information on the processes taking place in fine aerosols during different seasons at the
544 Central European station of Košetice. Seasonal variations were observed for $\delta^{13}\text{C}$ and $\delta^{15}\text{N}$, as well as
545 for TC and TN. The supporting data (i.e., ions, EC/OC, meteorology, trace gases) revealed characteristic
546 processes that led to changes in the isotopic compositions on the site.

547 The main and gradual changes in nitrogen isotopic composition occurred in spring. During early spring,
548 domestic heating with wood stoves is still common, with high nitrate concentrations in aerosols, which
549 decreased toward the end of spring. Additionally, temperature slowly increases, and the overall situation
550 leads to thermodynamic equilibrium exchange between gas (NO_{x3} - NH_3 - SO_2 mixture) and aerosol (NO_3^-
551 - NH_4^+ - SO_4^{2-} mixture) phases, which causes ^{15}N enrichment in aerosols. Enrichment of ^{15}N ($\Delta\delta^{15}\text{N}$)
552 from the beginning to the end of spring was approximately +10%. Gradual springtime changes in
553 isotopic composition were also observed for $\delta^{13}\text{C}$, but the depletion was small, and $\Delta\delta^{13}\text{C}$ was only -
554 1.4%.

555 In summer, we observed the lowest concentrations of TC and TN; however, there was an enhanced
556 enrichment of ^{15}N , which was probably caused by the aging of nitrogen aerosols, where ammonium
557 sulfate is subjected to isotopic fractionation via equilibrium exchange between $\text{NH}_3(\text{g})$ and $\text{NH}_4^+(\text{p})$.
558 Based on a $\text{NH}_4^+/\text{SO}_4^{2-}$ molar ratio of less than 2, we concluded that summer aerosols become more
559 acidic, and thus, kinetic isotopic fractionation took place via the equilibrium exchange of nitrogen
560 species. However, summer values of $\delta^{15}\text{N}$ were still among the highest compared with those in previous
561 studies, which can be explained by several factors. First, a fine aerosol fraction (PM1) is more reactive,
562 and its residence time in the atmosphere is longer than coarse mode, leading to ^{15}N enrichment in aged
563 aerosols. Second, summer aerosols, compared to other seasons, contain a negligible amount of nitrate,
564 contributing to a decrease in the average value of $\delta^{15}\text{N}$ of TN. On the other hand, we observed an
565 enrichment of ^{13}C only in summer, which can be explained by the photooxidation processes of organics
566 and is supported by the positive correlation of $\delta^{13}\text{C}$ with temperature and ozone. Despite this slow
567 enrichment process, summertime $\delta^{13}\text{C}$ values were the lowest compared to those in other seasons and
568 referred predominantly to organic aerosols of biogenic origin. The role of organics in summer may also
569 have an effect on the aforementioned ^{15}N enrichment due to thermodynamic equilibrium.

570 In winter, we found the highest concentrations of TC and TN. Lower winter $\delta^{15}\text{N}$ values were apparently
571 influenced by fresh aerosols from combustion, which were strongly driven by the amount of nitrates
572 (mainly NH_4NO_3 in PM1), and led to an average winter value of $\delta^{15}\text{N}$ approximately 14%. Winter $\delta^{13}\text{C}$
573 values were more enriched than summer values, and they were connected mainly to emissions from
574 coal and (mostly) biomass burning for domestic heating.

575 We observed an aerosol event in winter, which was characterized by temperatures below the freezing
576 point, stable southeast winds, and a unique isotope signature with a depletion of ^{15}N and enrichment of



577 ^{13}C . The winter *Event* characterized by ^{15}N depletion was probably caused by the dry deposition of NH_3
578 (with heavier isotope) during cold weather, and with decreasing concentrations of NO_3^- . However, it
579 was completely opposite to a summertime decrease in nitrate, which led to an enrichment of ^{15}N . In the
580 case of the most depleted ^{15}N event, nitrate was suppressed to partition in aerosol and gas phases with
581 unidirectional reactions of isotopically light ammonia and sulfuric acid resulting in $(\text{NH}_4)_2\text{SO}_4$, which
582 originated mainly from agriculture emissions in this case.

583 The majority the yearly data showed a strong correlation between $\delta^{15}\text{N}$ and ambient temperature,
584 demonstrating an enrichment of ^{15}N via isotopic equilibrium exchange between the gas and particulate
585 phases. This process seemed to be one of the main mechanisms for ^{15}N enrichment at the Košetice site,
586 especially during spring. The most ^{15}N -enriched summer and most ^{15}N -depleted winter samples were
587 limited by the partitioning of nitrate in aerosols and suppressed equilibrium exchange between gaseous
588 NH_3 and aerosol NH_4^+ .

589 This study revealed a picture of the seasonal cycle of $\delta^{15}\text{N}$ in aerosol TN at the Košetice site. In the case
590 of carbon, the seasonal cycle of $\delta^{13}\text{C}$ values was not so pronounced because they mainly depend on the
591 isotopic composition of primary sources, which often overlapped, and because secondary reactions
592 were influenced by the kinetic isotopic effect, while phase transfer probably did not play a crucial role.

593

594 **Acknowledgements**

595

596 This study was supported by funding from the Japan Society for the Promotion of Science (JSPS)
597 through Grant-in-Aid No. 24221001, from the Ministry of Education, Youth and Sports of the Czech
598 Republic under the project No. LM2015037 and under the grant ACTRIS-CZ RI
599 (CZ.02.1.01/0.0/0.0/16_013/0001315). We also thank the Czech Hydrometeorological Institute for
600 providing its meteorological data and Dr. Milan Váňa and his colleagues from the Košetice Observatory
601 for their valuable cooperation during the collection of samples. We appreciate the financial support of
602 the JSPS fellowship to P. Vodička (P16760).

603

604 **References:**

605

606 Aggarwal, S. G., Kawamura, K., Umarji, G. S., Tachibana, E., Patil, R. S. and Gupta, P. K.: Organic
607 and inorganic markers and stable C-, N-isotopic compositions of tropical coastal aerosols from
608 megacity Mumbai: Sources of organic aerosols and atmospheric processing, Atmos. Chem. Phys.,
609 13(9), 4667–4680, doi:10.5194/acp-13-4667-2013, 2013.

610 Agnihotri, R., Mandal, T. K., Karapurkar, S. G., Naja, M., Gadi, R., Ahammed, Y. N., Kumar, A.,
611 Saud, T. and Saxena, M.: Stable carbon and nitrogen isotopic composition of bulk aerosols over India
612 and northern Indian Ocean, Atmos. Environ., 45(17), 2828–2835,
613 doi:10.1016/j.atmosenv.2011.03.003, 2011.

614 Beyn, F., Matthias, V., Aulinger, A. and Dähnke, K.: Do N-isotopes in atmospheric nitrate deposition
615 reflect air pollution levels?, Atmos. Environ., 107, 281–288, doi:10.1016/j.atmosenv.2015.02.057,



- 616 2015.
- 617 Bikkina, S., Kawamura, K. and Sarin, M.: Stable carbon and nitrogen isotopic composition of fine
618 mode aerosols (PM_{2.5}) over the Bay of Bengal: impact of continental sources, *Tellus B Chem. Phys.*
619 *Meteorol.*, 68(1), 31518, doi:10.3402/tellusb.v68.31518, 2016.
- 620 Cachier, H.: Isotopic characterization of carbonaceous aerosols, *Aerosol Sci. Technol.*, 10(2), 379–
621 385, doi:10.1080/02786828908959276, 1989.
- 622 Cavalli, F., Viana, M., Yttri, K. E., Genberg, J. and Putaud, J.-P.: Toward a standardised thermal-
623 optical protocol for measuring atmospheric organic and elemental carbon: the EUSAAR protocol,
624 *Atmos. Meas. Tech.*, 3(1), 79–89, doi:10.5194/amt-3-79-2010, 2010.
- 625 Ceburnis, D., Masalaite, A., Ovadnevaite, J., Garbaras, A., Remeikis, V., Maenhaut, W., Claeys, M.,
626 Sciare, J., Baisnée, D. and O’Dowd, C. D.: Stable isotopes measurements reveal dual carbon pools
627 contributing to organic matter enrichment in marine aerosol, *Sci. Rep.*, 6(July), 1–6,
628 doi:10.1038/srep36675, 2016.
- 629 Ciężka, M., Modelska, M., Górka, M., Trojanowska-Olichwer, A. and Widory, D.: Chemical and
630 isotopic interpretation of major ion compositions from precipitation: A one-year temporal monitoring
631 study in Wrocław, SW Poland, *J. Atmos. Chem.*, 73, 61–80, doi:10.1007/s10874-015-9316-2, 2016.
- 632 Dean, J. R., Leng, M. J. and Mackay, A. W.: Is there an isotopic signature of the Anthropocene?,
633 *Anthr. Rev.*, 1(3), 276–287, doi:10.1177/2053019614541631, 2014.
- 634 Felix, D. J., Elliott, E. M., Gish, T. J., McConnell, L. L. and Shaw, S. L.: Characterizing the isotopic
635 composition of atmospheric ammonia emission sources using passive samplers and a combined
636 oxidation-bacterial denitrifier approach, *Rapid Commun. Mass Spectrom.*, 27(20), 2239–2246,
637 doi:10.1002/rcm.6679, 2013.
- 638 Felix, J. D., Elliott, E. M. and Shaw, S. L.: Nitrogen isotopic composition of coal-fired power plant
639 NO_x: Influence of emission controls and implications for global emission inventories, *Environ. Sci.*
640 *Technol.*, 46(6), 3528–3535, doi:10.1021/es203355v, 2012.
- 641 Fisseha, R., Saurer, M., Jäggi, M., Siegwolf, R. T. W., Dommen, J., Szidat, S., Samburova, V. and
642 Baltensperger, U.: Determination of primary and secondary sources of organic acids and
643 carbonaceous aerosols using stable carbon isotopes, *Atmos. Environ.*, 43(2), 431–437,
644 doi:10.1016/j.atmosenv.2008.08.041, 2009a.
- 645 Fisseha, R., Spahn, H., Wegener, R., Hohaus, T., Brasse, G., Wissel, H., Tillmann, R., Wahner, A.,
646 Koppmann, R. and Kiendler-Scharr, A.: Stable carbon isotope composition of secondary organic
647 aerosol from β -pinene oxidation, *J. Geophys. Res.*, 114(D2), D02304, doi:10.1029/2008JD011326,
648 2009b.
- 649 Freyer, H. D.: Seasonal variation of ¹⁵N/¹⁴N ratios in atmospheric nitrate species, *Tellus B*, 43(1),
650 30–44, doi:10.1034/j.1600-0889.1991.00003.x, 1991.
- 651 Freyer, H. D., Kley, D., Volz-Thomas, A. and Kobel, K.: On the interaction of isotopic exchange
652 processes with photochemical reactions in atmospheric oxides of nitrogen, *J. Geophys. Res.*, 98(D8),
653 14791–14796, doi:10.1029/93JD00874, 1993.
- 654 Fuzzi, S., Baltensperger, U., Carslaw, K., Decesari, S., Denier Van Der Gon, H., Facchini, M. C.,
655 Fowler, D., Koren, I., Langford, B., Lohmann, U., Nemitz, E., Pandis, S., Riipinen, I., Rudich, Y.,
656 Schaap, M., Slowik, J. G., Spracklen, D. V., Vignati, E., Wild, M., Williams, M. and Gilardoni, S.:
657 Particulate matter, air quality and climate: Lessons learned and future needs, *Atmos. Chem. Phys.*,
658 15(14), 8217–8299, doi:10.5194/acp-15-8217-2015, 2015.
- 659 Gensch, I., Kiendler-Scharr, A. and Rudolph, J.: Isotope ratio studies of atmospheric organic
660 compounds: Principles, methods, applications and potential, *Int. J. Mass Spectrom.*, 365–366, 206–
661 221, doi:10.1016/j.jjms.2014.02.004, 2014.



- 662 Górká, M., Rybicki, M., Simoneit, B. R. T. and Marynowski, L.: Determination of multiple organic
663 matter sources in aerosol PM10 from Wrocław, Poland using molecular and stable carbon isotope
664 compositions, *Atmos. Environ.*, 89, 739–748, doi:10.1016/j.atmosenv.2014.02.064, 2014.
- 665 Harrison, R. M. and Pio, C. A.: Size-differentiated composition of inorganic atmospheric aerosols of
666 both marine and polluted continental origin, *Atmos. Environ.*, 17(9), 1733–1738, doi:10.1016/0004-
667 6981(83)90180-4, 1983.
- 668 Heaton, T. H. E.: 15N/14N ratios of NOx from vehicle engines and coal-fired power stations, *Tellus*
669 B, 42, 304–307, 1990.
- 670 Heaton, T. H. E., Spiro, B. and Robertson, S. M. C.: Potential canopy influences on the isotopic
671 composition of nitrogen and sulphur in atmospheric deposition, *Oecologia*, (109), 600–607, 1997.
- 672 Hyslop, N. P.: Impaired visibility: the air pollution people see, *Atmos. Environ.*, 43(1), 182–195,
673 doi:10.1016/j.atmosenv.2008.09.067, 2009.
- 674 Jickells, T., Baker, A. R., Cape, J. N., Cornell, S. E. and Nemitz, E.: The cycling of organic nitrogen
675 through the atmosphere., *Philos. Trans. R. Soc. Lond. B. Biol. Sci.*, 368(1621), 20130115,
676 doi:10.1098/rstb.2013.0115, 2013.
- 677 Kawamura, K., Kobayashi, M., Tsubonuma, N., Mochida, M., Watanabe, T. and Lee, M.: Organic
678 and inorganic compositions of marine aerosols from East Asia: Seasonal variations of water-soluble
679 dicarboxylic acids, major ions, total carbon and nitrogen, and stable C and N isotopic composition,
680 *Geochemical Soc. Spec. Publ.*, 9(C), 243–265, doi:10.1016/S1873-9881(04)80019-1, 2004.
- 681 Kawashima, H. and Kurahashi, T.: Inorganic ion and nitrogen isotopic compositions of atmospheric
682 aerosols at Yurihonjo, Japan: Implications for nitrogen sources, *Atmos. Environ.*, 45(35), 6309–6316,
683 doi:10.1016/j.atmosenv.2011.08.057, 2011.
- 684 Kundu, S., Kawamura, K. and Lee, M.: Seasonal variation of the concentrations of nitrogenous
685 species and their nitrogen isotopic ratios in aerosols at Gosan, Jeju Island: Implications for
686 atmospheric processing and source changes of aerosols, *J. Geophys. Res. Atmos.*, 115(20), 1–19,
687 doi:10.1029/2009JD013323, 2010.
- 688 Kunwar, B., Kawamura, K. and Zhu, C.: Stable carbon and nitrogen isotopic compositions of ambient
689 aerosols collected from Okinawa Island in the western North Pacific Rim, an outflow region of Asian
690 dusts and pollutants, *Atmos. Environ.*, 131, 243–253, doi:10.1016/j.atmosenv.2016.01.035, 2016.
- 691 Li, D. and Wang, X.: Nitrogen isotopic signature of soil-released nitric oxide (NO) after fertilizer
692 application, *Atmos. Environ.*, 42(19), 4747–4754, doi:10.1016/j.atmosenv.2008.01.042, 2008.
- 693 Liggio, J., Li, S. M., Vlasenko, A., Stroud, C. and Makar, P.: Depression of ammonia uptake to
694 sulfuric acid aerosols by competing uptake of ambient organic gases, *Environ. Sci. Technol.*, 45(7),
695 2790–2796, doi:10.1021/es103801g, 2011.
- 696 Martinelli, L. A., Camargo, P. B., Lara, L. B. L. S., Victoria, R. L. and Artaxo, P.: Stable carbon and
697 nitrogen isotopic composition of bulk aerosol particles in a C4 plant landscape of southeast Brazil,
698 *Atmos. Environ.*, 36(14), 2427–2432, doi:10.1016/S1352-2310(01)00454-X, 2002.
- 699 Martinsson, J., Andersson, A., Sporre, M. K., Friberg, J., Kristensson, A., Swietlicki, E., Olsson, P. A.
700 and Stenström, K. E.: Evaluation of $\delta^{13}\text{C}$ in carbonaceous aerosol source apportionment at a rural
701 measurement site, *Aerosol Air Qual. Res.*, 17, 2081–2094, doi:10.4209/aaqr.2016.09.0392, 2017.
- 702 Masalaite, A., Remeikis, V., Garbaras, A., Dudoitis, V., Ulevicius, V. and Ceburnis, D.: Elucidating
703 carbonaceous aerosol sources by the stable carbon $\delta^{13}\text{C}_{\text{TC}}$ ratio in size-segregated particles, *Atmos.*
704 *Res.*, 158–159, 1–12, doi:10.1016/j.atmosres.2015.01.014, 2015.
- 705 Masalaite, A., Holzinger, R., Remeikis, V., Röckmann, T. and Dusek, U.: Characteristics, sources and
706 evolution of fine aerosol (PM1) at urban, coastal and forest background sites in Lithuania, *Atmos.*



- 707 Environ., 148, 62–76, doi:10.1016/j.atmosenv.2016.10.038, 2017.
- 708 Mbengue, S., Fusek, M., Schwarz, J., Vodička, P., Šmejkalová, A. H. and Holoubek, I.: Four years of
709 highly time resolved measurements of elemental and organic carbon at a rural background site in
710 Central Europe, Atmos. Environ., 182, 335–346, doi:10.1016/j.atmosenv.2018.03.056, 2018.
- 711 Mkoma, S., Kawamura, K., Tachibana, E. and Fu, P.: Stable carbon and nitrogen isotopic
712 compositions of tropical atmospheric aerosols: sources and contribution from burning of C3 and C4
713 plants to organic aerosols, Tellus B, 66, 20176, doi:10.3402/tellusb.v66.20176, 2014.
- 714 Neff, J. C., Holland, E. A., Dentener, F. J., McDowell, W. H. and Russell, K. M.: The origin,
715 composition and rates of organic nitrogen deposition: a missing piece of the nitrogen cycle?,
716 Biogeochemistry, 57/58, 99–136, 2002.
- 717 Park, Y., Park, K., Kim, H., Yu, S., Noh, S., Kim, M., Kim, J., Ahn, J., Lee, M., Seok, K. and Kim,
718 Y.: Characterizing isotopic compositions of TC-C, NO₃-N, and NH₄⁺-N in PM_{2.5} in South Korea:
719 Impact of China's winter heating, Environ. Pollut., 233, 735–744, doi:10.1016/j.envpol.2017.10.072,
720 2018.
- 721 Pavuluri, C. M. and Kawamura, K.: Seasonal changes in TC and WSOC and their ¹³C isotope ratios
722 in Northeast Asian aerosols: land surface–biosphere–atmosphere interactions, Acta Geochim., 36(3),
723 355–358, doi:10.1007/s11631-017-0157-3, 2017.
- 724 Pavuluri, C. M., Kawamura, K., Tachibana, E. and Swaminathan, T.: Elevated nitrogen isotope ratios
725 of tropical Indian aerosols from Chennai: Implication for the origins of aerosol nitrogen in South and
726 Southeast Asia, Atmos. Environ., 44(29), 3597–3604, doi:10.1016/j.atmosenv.2010.05.039, 2010.
- 727 Pavuluri, C. M., Kawamura, K. and Fu, P. Q.: Atmospheric chemistry of nitrogenous aerosols in
728 northeastern Asia: Biological sources and secondary formation, Atmos. Chem. Phys., 15(17), 9883–
729 9896, doi:10.5194/acp-15-9883-2015, 2015a.
- 730 Pavuluri, C. M., Kawamura, K. and Swaminathan, T.: Time-resolved distributions of bulk parameters,
731 diacids, ketoacids and α -dicarbonyls and stable carbon and nitrogen isotope ratios of TC and TN in
732 tropical Indian aerosols: Influence of land/sea breeze and secondary processes, Atmos. Res., 153,
733 188–199, doi:10.1016/j.atmosres.2014.08.011, 2015b.
- 734 Pichlmayer, F., Schöner, W., Seibert, P., Stichler, W. and Wagenbach, D.: Stable isotope analysis for
735 characterization of pollutants at high elevation alpine sites, Atmos. Environ., 32(23), 4075–4085,
736 doi:10.1016/S1352-2310(97)00405-6, 1998.
- 737 Pokorná, P., Schwarz, J., Krejci, R., Swietlicki, E., Havránek, V. and Ždímal, V.: Comparison of
738 PM_{2.5} chemical composition and sources at a rural background site in Central Europe between
739 1993/1994/1995 and 2009/2010: Effect of legislative regulations and economic transformation on the
740 air quality, Environ. Pollut., 241, 841–851, doi:10.1016/j.envpol.2018.06.015, 2018.
- 741 Savard, M. M., Cole, A., Smirnoff, A. and Vet, R.: $\Delta^{15}\text{N}$ values of atmospheric N species
742 simultaneously collected using sector-based samplers distant from sources – Isotopic inheritance and
743 fractionation, Atmos. Environ., 162, 11–22, doi:10.1016/j.atmosenv.2017.05.010, 2017.
- 744 Schwarz, J., Cusack, M., Karban, J., Chalupníčková, E., Havránek, V., Smolík, J. and Ždímal, V.:
745 PM_{2.5} chemical composition at a rural background site in Central Europe, including correlation and
746 air mass back trajectory analysis, Atmos. Res., 176–177, 108–120,
747 doi:10.1016/j.atmosres.2016.02.017, 2016.
- 748 Silvern, R. F., Jacob, D. J., Kim, P. S., Marais, E. A., Turner, J. R., Campuzano-Jost, P. and Jimenez,
749 J. L.: Inconsistency of ammonium-sulfate aerosol ratios with thermodynamic models in the eastern
750 US: A possible role of organic aerosol, Atmos. Chem. Phys., 17(8), 5107–5118, doi:10.5194/acp-17-
751 5107-2017, 2017.
- 752 Skipitytė, R., Mašalaitė, A., Garbaras, A., Mickienė, R., Ragažinskienė, O., Baliukonienė, V.,



- 753 Bakutis, B., Štugždaitė, J., Petkevičius, S., Maruška, A. S. and Remeikis, V.: Stable isotope ratio
754 method for the characterisation of the poultry house environment, *Isotopes Environ. Health Stud.*,
755 53(3), 243–260, doi:10.1080/10256016.2016.1230609, 2016.
- 756 Stein, A. F., Draxler, R. R., Rolph, G. D., Stunder, B. J. B., Cohen, M. D. and Ngan, F.: NOAA's
757 hysplit atmospheric transport and dispersion modeling system, *Bull. Am. Meteorol. Soc.*, 96(12),
758 2059–2077, doi:10.1175/BAMS-D-14-00110.1, 2015.
- 759 Stelson, A. W., Friedlander, S. K. and Seinfeld, J. H.: A note on the equilibrium relationship between
760 ammonia and nitric acid and particulate ammonium nitrate, *Atmos. Environ.*, 13(3), 369–371,
761 doi:10.1016/0004-6981(79)90293-2, 1979.
- 762 Váňa, M. and Dvorská, A.: Košetice Observatory - 25 years, 1. edition., Czech Hydrometeorological
763 Institute, Prague., 2014.
- 764 Vodička, P., Schwarz, J., Cusack, M. and Ždímal, V.: Detailed comparison of OC/EC aerosol at an
765 urban and a rural Czech background site during summer and winter, *Sci. Total Environ.*, 518–519(2),
766 424–433, doi:10.1016/j.scitotenv.2015.03.029, 2015.
- 767 Walters, W. W., Simonini, D. S. and Michalski, G.: Nitrogen isotope exchange between NO and NO
768 2 and its implications for $\delta^{15}\text{N}$ variations in tropospheric NO_x and atmospheric nitrate, *Geophys.*
769 *Res. Lett.*, (2), 1–26, doi:10.1002/2015GL066438, 2015a.
- 770 Walters, W. W., Goodwin, S. R. and Michalski, G.: Nitrogen stable isotope composition ($\delta^{15}\text{N}$) of
771 vehicle-emitted NO_x, *Environ. Sci. Technol.*, 49(4), 2278–2285, doi:10.1021/es505580v, 2015b.
- 772 Wang, G., Xie, M., Hu, S., Gao, S., Tachibana, E. and Kawamura, K.: Dicarboxylic acids, metals and
773 isotopic compositions of C and N in atmospheric aerosols from inland China: Implications for dust
774 and coal burning emission and secondary aerosol formation, *Atmos. Chem. Phys.*, 10(13), 6087–
775 6096, doi:10.5194/acp-10-6087-2010, 2010.
- 776 Wang, Y. L., Liu, X. Y., Song, W., Yang, W., Han, B., Dou, X. Y., Zhao, X. D., Song, Z. L., Liu, C.
777 Q. and Bai, Z. P.: Source appointment of nitrogen in PM_{2.5} based on bulk $\delta^{15}\text{N}$ signatures and a
778 Bayesian isotope mixing model, *Tellus, Ser. B Chem. Phys. Meteorol.*, 69(1), 1–10,
779 doi:10.1080/16000889.2017.1299672, 2017.
- 780 Widory, D.: Combustibles, fuels and their combustion products: A view through carbon isotopes,
781 *Combust. Theory Model.*, 10(5), 831–841, doi:10.1080/13647830600720264, 2006.
- 782 Widory, D.: Nitrogen isotopes: Tracers of origin and processes affecting PM₁₀ in the atmosphere of
783 Paris, *Atmos. Environ.*, 41(11), 2382–2390, doi:10.1016/j.atmosenv.2006.11.009, 2007.
- 784 Widory, D., Roy, S., Le Moullec, Y., Goupil, G., Cocherie, A. and Guerrot, C.: The origin of
785 atmospheric particles in Paris: A view through carbon and lead isotopes, *Atmos. Environ.*, 38(7),
786 953–961, doi:10.1016/j.atmosenv.2003.11.001, 2004.
- 787 Yeatman, S. G., Spokes, L. J., Dennis, P. F. and Jickells, T. D.: Can the study of nitrogen isotopic
788 composition in size-segregated aerosol nitrate and ammonium be used to investigate atmospheric
789 processing mechanisms?, *Atmos. Environ.*, 35(7), 1337–1345, doi:10.1016/S1352-2310(00)00457-X,
790 2001a.
- 791 Yeatman, S. G., Spokes, L. J., Dennis, P. F. and Jickells, T. D.: Comparisons of aerosol nitrogen
792 isotopic composition at two polluted coastal sites, *Atmos. Environ.*, 35(7), 1307–1320,
793 doi:10.1016/S1352-2310(00)00408-8, 2001b.
- 794 Zíková, N. and Ždímal, V.: Long-term measurement of aerosol number size distributions at rural
795 background station Košetice, *Aerosol Air Qual. Res.*, 13(5), 1464–1474,
796 doi:10.4209/aaqr.2013.02.0056, 2013.
- 797



798

799

800

801 **Tables:**

802

803 Table 1: Seasonal and entire campaign averages \pm standard deviations, (medians in brackets) of
804 different variables.

	Autumn	Winter	Spring	Summer	Year
N of samples	25	45	43	33	146
TC [$\mu\text{g m}^{-3}$] (from EA)	3.61 \pm 1.61 (3.30)	4.76 \pm 2.44 (3.88)	3.78 \pm 2.03 (3.04)	2.71 \pm 0.76 (2.68)	3.81 \pm 2.03 (3.35)
TN [$\mu\text{g m}^{-3}$]	1.56 \pm 1.18 (1.33)	1.67 \pm 0.96 (1.45)	2.00 \pm 1.62 (1.47)	0.81 \pm 0.29 (0.82)	1.56 \pm 1.22 (1.26)
$\delta^{13}\text{C}$ [‰]	-26.8 \pm 0.5 (-26.9)	-26.7 \pm 0.5 (-26.7)	-27.1 \pm 0.5 (-27.0)	-27.8 \pm 0.4 (-27.7)	-27.1 \pm 0.6 (-27.0)
$\delta^{15}\text{N}$ [‰]	17.1 \pm 2.4 (16.9)	13.1 \pm 4.5 (15.2)	17.6 \pm 3.5 (17.3)	25.0 \pm 1.6 (25.1)	17.8 \pm 5.5 (16.9)
TC/PM1 [%]	28 \pm 6 (26)	33 \pm 8 (32)	38 \pm 15 (35)	31 \pm 6 (30)	33 \pm 11 (31)
TN/PM1 [%]	11 \pm 3 (11)	11 \pm 3 (12)	17 \pm 4 (17)	9 \pm 2 (9)	12 \pm 4 (12)
NO₃⁻-N/TN [%]	21 \pm 6 (21)	25 \pm 8 (28)	22 \pm 8 (21)	5 \pm 3 (4)	19 \pm 10 (20)
NH₄⁺-N/TN [%]	51 \pm 6 (51)	51 \pm 9 (49)	58 \pm 7 (60)	57 \pm 6 (57)	54 \pm 8 (54)
OrgN/TN [%]	28 \pm 8 (26)	25 \pm 8 (23)	20 \pm 8 (19)	39 \pm 6 (38)	27 \pm 10 (25)
TC/TN	2.77 \pm 1.10 (2.60)	3.34 \pm 1.66 (2.68)	2.33 \pm 0.98 (2.34)	3.60 \pm 1.23 (3.45)	3.01 \pm 1.38 (2.61)

805

806

807

808

809

810

811

812

813

814

815

816

817



818

819

820

821

822 Table 2: Spearman correlation coefficients (r) of $\delta^{15}\text{N}$ with various tracers. Only bold values are
823 statistically significant (p -values < 0.05).

$\delta^{15}\text{N}$ vs.	Autumn	Winter*	Spring	Summer	Year*	Event
TN	-0.30	-0.40	-0.70	0.36	-0.54	0.93
TN/PM1	-0.63	-0.50	-0.02	0.37	-0.35	0.36
NO_3^- -N/TN	-0.39	-0.04	-0.73	-0.26	-0.77	0.98
NH_4^+ -N/TN	0.16	-0.30	0.60	0.52	0.42	-0.86
OrgN/TN	0.20	0.38	0.20	-0.33	0.51	-0.71
NO_3^-	-0.41	-0.35	-0.80	-0.03	-0.78	0.96
NH_4^+	-0.22	-0.42	-0.61	0.40	-0.44	0.75
OrgN	-0.26	-0.27	-0.56	0.30	-0.25	0.71
SO_4^{2-}	-0.07	-0.38	-0.30	0.51	0.03	-0.57
Cl^-	-0.37	-0.18	-0.74	-0.37	-0.74	0.99
O_3 (gas)	0.45	0.14	0.15	-0.02	0.40	-0.71
NO_2 (gas)	-0.53	-0.34	-0.72	0.20	-0.64	0.86
NO_2/NO (gas)	-0.51	-0.26	-0.82	0.14	-0.76	0.82
Temp.	0.58	0.30	0.52	-0.21	0.77	-0.43

824 *Event data are excluded from winter and year datasets.

825

826

827

828

829

830

831

832

833

834

835

836

837

838

839

840



841

842

843

844

845 Table 3: Spearman correlation coefficients (r) of $\delta^{13}\text{C}$ with various tracers. Only bold values are
846 statistically significant (p -values < 0.05).

$\delta^{13}\text{C}$ vs.	Autumn	Winter*	Spring	Summer	Year*	Event
OC	0.64	0.63	0.91	0.39	0.75	0.75
EC	0.61	0.74	0.88	0.28	0.84	0.46
EC/TC	0.06	0.06	0.13	-0.51	0.32	-0.32
TC/PM1	-0.16	-0.05	-0.40	0.22	-0.09	0.32
NO_3^-	0.74	0.52	0.71	0.12	0.76	0.39
NH_4^+	0.84	0.59	0.80	0.42	0.66	0.75
Oxalate	0.34	0.62	0.71	0.65	0.25	0.93
SO_4^{2-}	0.80	0.64	0.73	0.41	0.34	0.54
K^+	0.84	0.63	0.70	0.47	0.76	0.93
Cl^-	0.44	0.62	0.68	0.44	0.76	0.25
CO (gas)	0.21	0.53	0.60	0.32	0.37	0.68
O_3 (gas)	-0.41	-0.26	0.14	0.66	-0.33	0.11
NO_2 (gas)	0.67	0.38	0.70	0.18	0.69	0.32
NO_2/NO (gas)	0.72	0.65	0.67	0.68	0.78	0.96
Temp.	-0.33	-0.35	-0.20	0.39	-0.57	-0.79

847 *Event data are excluded from winter and year datasets.

848

849

850

851

852

853

854

855

856

857

858

859

860

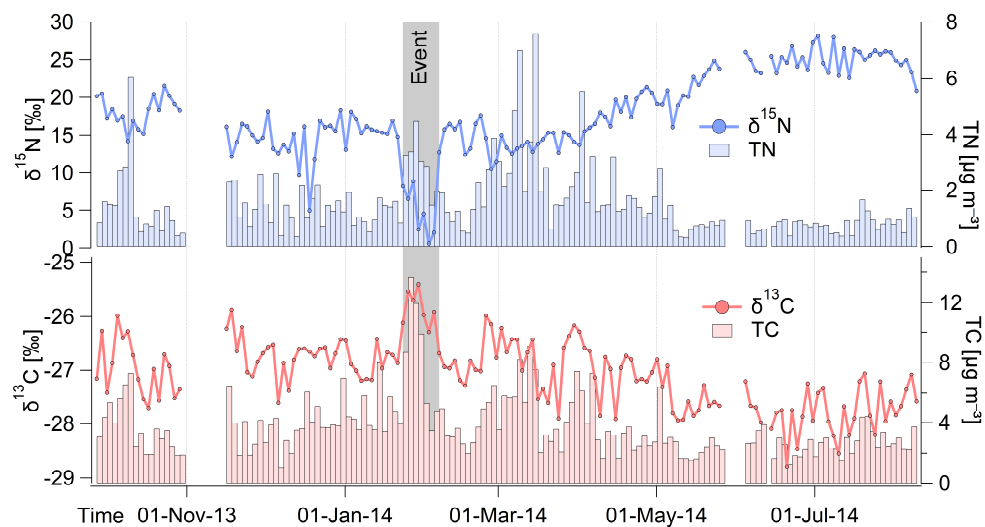
861

862

863

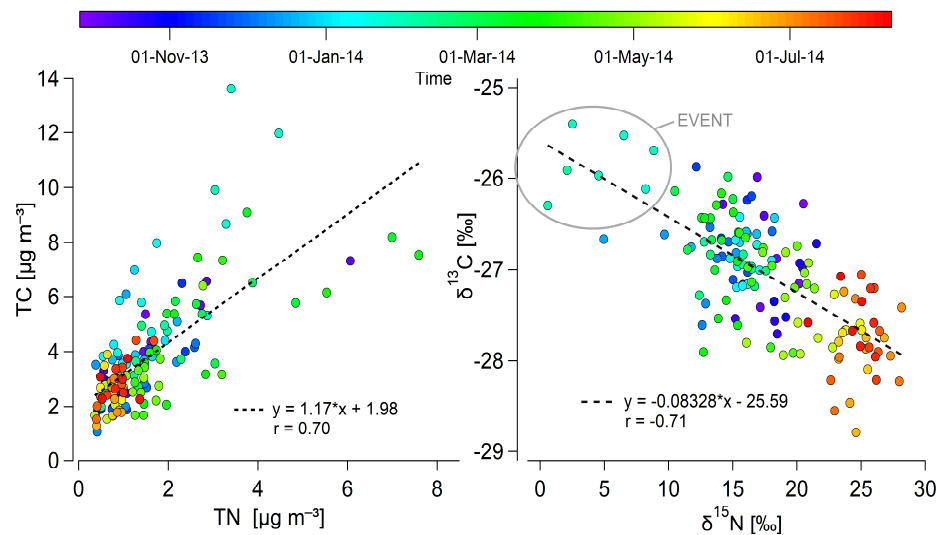


864 **Figures:**



865

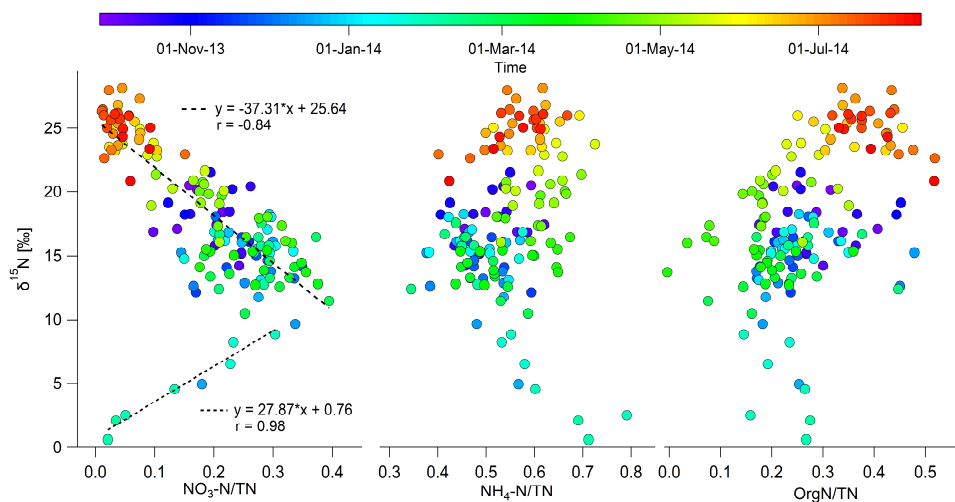
866 Fig. 1: Time series of $\delta^{15}\text{N}$ together with TN (top) and $\delta^{13}\text{C}$ together with TC (bottom) in PM1 aerosols
 867 at the Košice station. The gray color highlights an *Event* with divergent values, especially for $\delta^{15}\text{N}$.



868

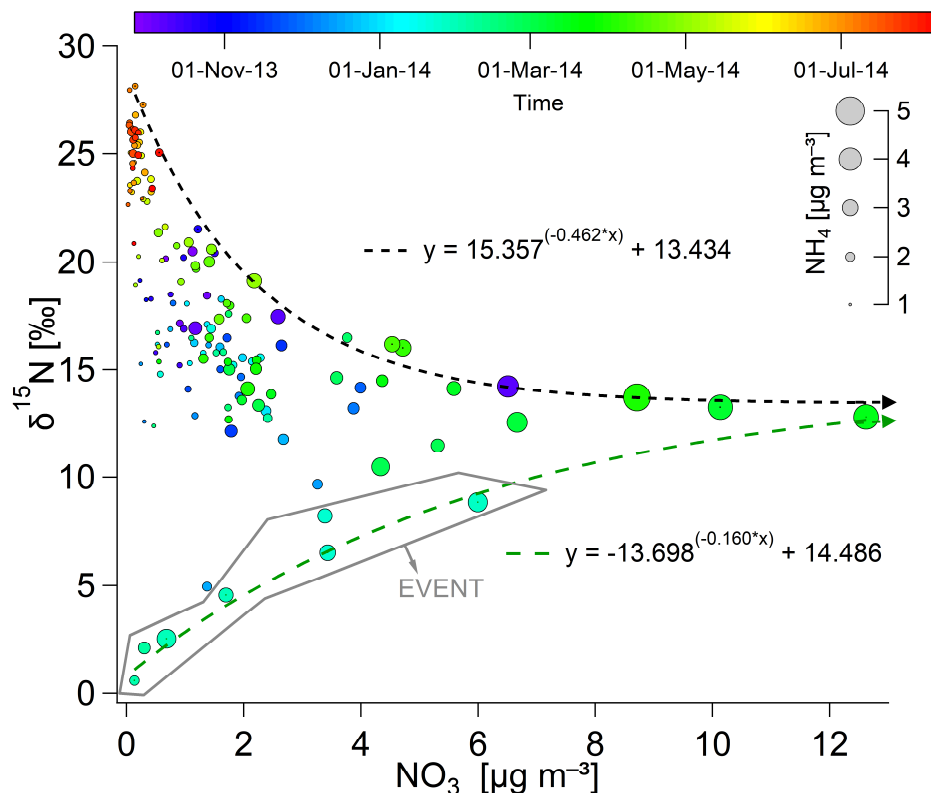
869 Fig. 2: Relationships between TC and TN (left) and their stable carbon and nitrogen isotopes (right).
 870 The color scale reflects the time of sample collection. The gray circle highlights the winter *Event*
 871 measurements.

872



873
 874
 875
 876

Fig. 3: Changes in $\delta^{15}\text{N}$ depending on fraction of individual nitrogen components ($\text{NO}_3\text{-N}$, $\text{NH}_4\text{-N}$, and OrgN) in TN. The color scale reflects the time of sample collection.

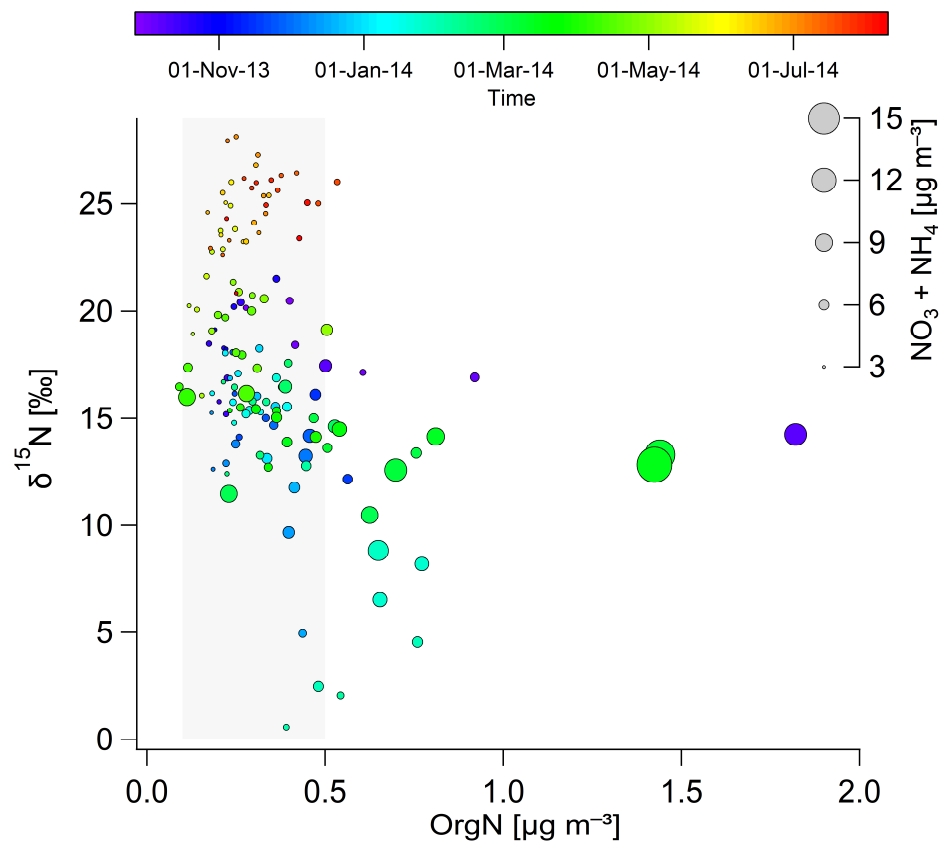


877
 878
 879
 880

Fig. 4: Relationships of $\delta^{15}\text{N}$ in TN vs. NO_3^- concentrations. The larger circles indicate higher NH_4^+ concentrations. The color scale reflects the time of sample collection.

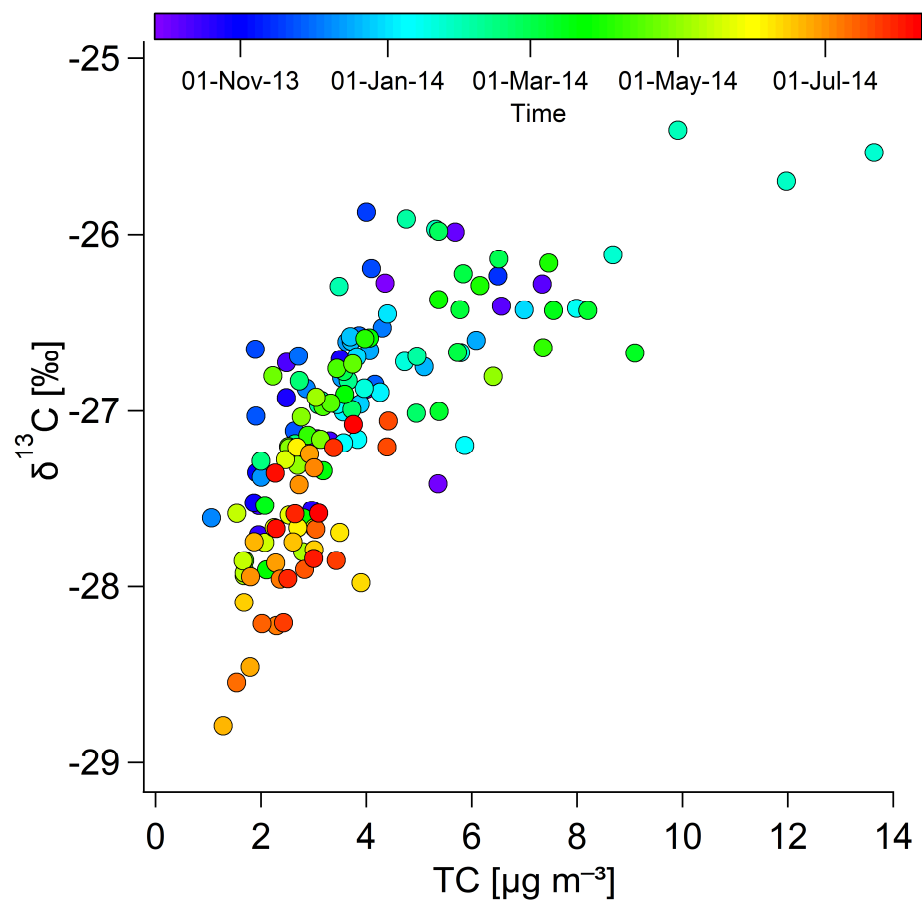


881



882

883 Fig. 5: Relationships of $\delta^{15}\text{N}$ in TN vs. OrgN concentrations. The larger circles indicate higher sums of
884 $\text{NO}_3 + \text{NH}_4$ concentrations. The color scale reflects the time of sample collection, and the highlighted
885 portion is a concentration range between 0.1-0.5 $\mu\text{g m}^{-3}$.

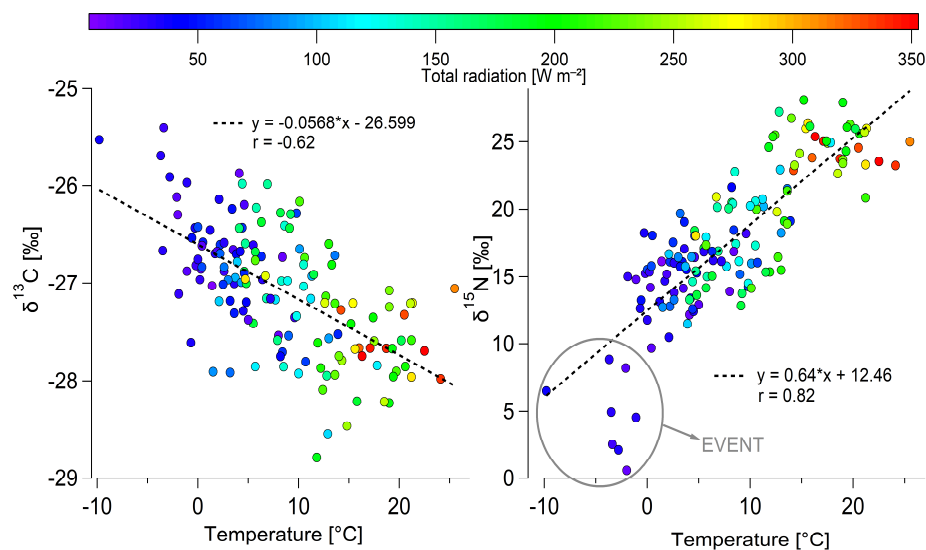


886

887

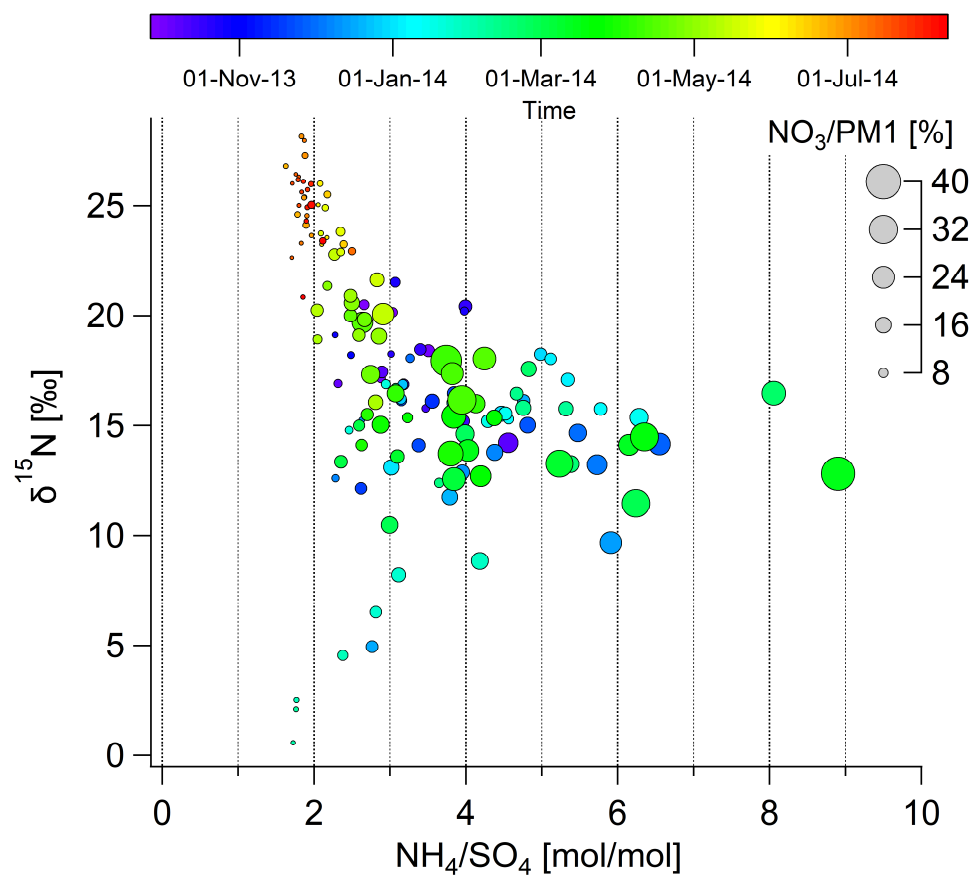
888

Fig. 6: Relationship between TC and $\delta^{13}\text{C}$. The color scale reflects the time of sample collection.



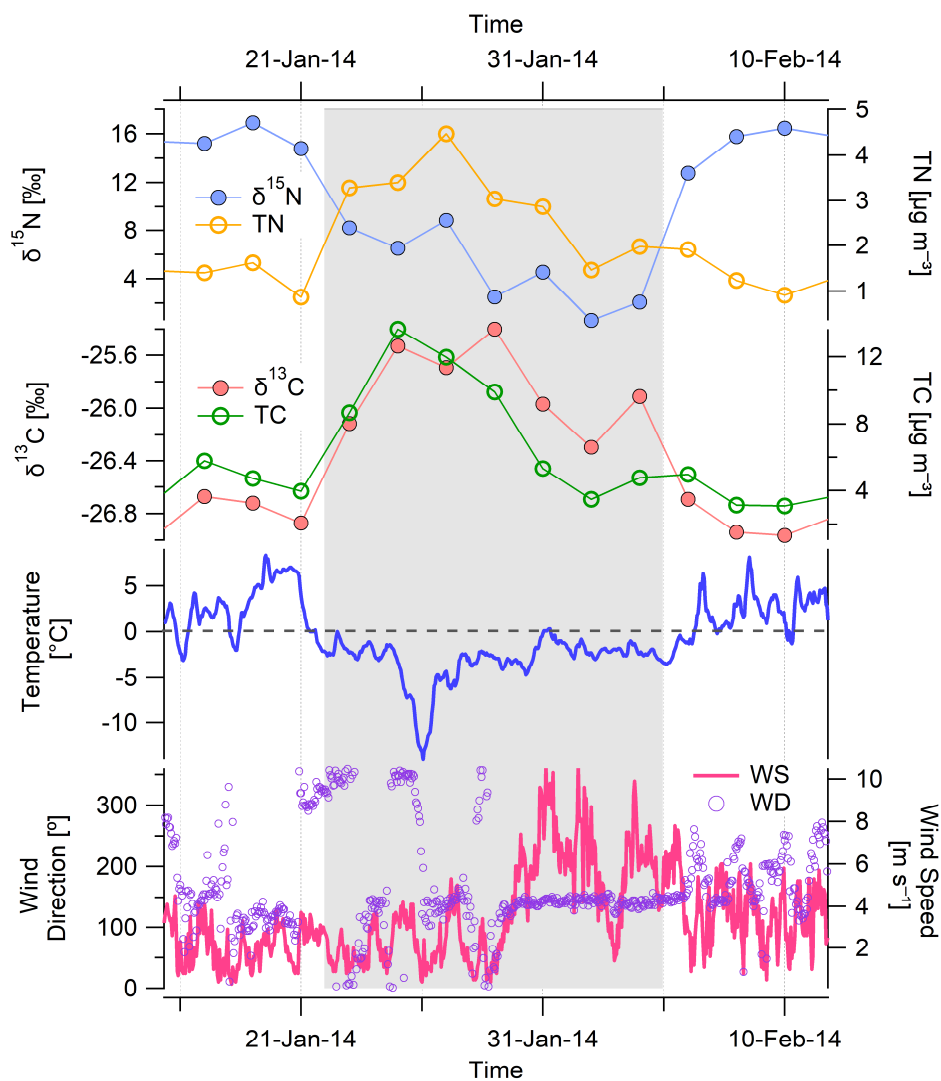
889

890 Fig. 7: Relationships between temperature and $\delta^{13}\text{C}$ in TC (left) and $\delta^{15}\text{N}$ in TN (right). The color scale
891 reflects the total radiation.



892

893 Fig. 8: Relationships between $\delta^{15}\text{N}$ in TN and molar ratios of $\text{NH}_4^+/\text{SO}_4^{2-}$ in particles. The larger circle
894 indicates a higher nitrate content in PM1. The color scale reflects the time of sample collection.



895
896 Fig. 9: Time series of $\delta^{15}\text{N}$, TN, $\delta^{13}\text{C}$, TC and meteorological variables (temperature, wind speed and
897 direction, 1 h time resolution) during the *Event*, which is highlighted by a gray color.
898

